Contribution from the Department of Chemistry, The University of Michigan, Ann Arbor, Michigan 48109, and Nuclear Research Center "Demokritos", Aghia Paraskevi, Attiki, Greece

Synthesis, Structural Characterization, and Electronic Properties of the [Fe$_6$S$_6$X$_6$(M(CO)$_3$)$_2$]$^{n-}$ Anions (M = Mo, W; n = 3, 4; X = Cl, Br, I). Heteronuclear Clusters of Possible Structural Relevance to the Fe/Mo/S Center in Nitrogenase

D. Coucouvanis,*,[1a] A. Salifoglou,[1a] M. G. Kanatzidis,[1a] W. R. Dunham,[1a] A. Simopoulos,[1b] and A. Kostikas[1b]

The synthesis and spectroscopic characterization of the [Fe$_6$S$_6$X$_6$(M(CO)$_3$)$_2$]$^{n-}$ clusters (M = Mo, X = Cl$^-$, Br$^-$, I$^-$, n = 3, 4; M = W, X = Cl$^-$, Br$^-$, n = 3) are reported. The crystal and molecular structures of (Et$_4$N)$_4$Fe$_6$S$_6$Cl$_6$[Mo(CO)$_3$]$_2$·2CH$_3$CN (I), (Ph$_4$P)$_4$Fe$_6$S$_6$Cl$_6$[Mo(CO)$_3$]$_2$·2CH$_3$CN (II), (Et$_4$N)$_3$Fe$_6$S$_6$Cl$_6$[Mo(CO)$_3$]$_2$ (III), and (Et$_4$N)$_3$Fe$_6$S$_6$Br$_6$[Mo(CO)$_3$]$_2$ (B, IV) are described in detail. I crystallizes in the monoclinic space group $P2_1/n$ with cell dimensions a = 13.192 (2) Å, b = 16.504 (5) Å, c = 16.080 (4) Å, β = 97.97 (2)°, and Z = 2. II crystallizes in the monoclinic space group $P2_1/n$ with cell dimensions a = 16.329 (6) Å, b = 16.253 (6) Å, c = 20.588 (5) Å, β = 94.97 (3)°, and Z = 2. III crystallizes in the rhombohedral space group $R\bar{3}c$ with cell dimensions a = b = c = 14.073 (2) Å, α = β = γ = 93.11 (1)°, and Z = 2. IV (B) crystallizes in the monoclinic space group $P2_1/n$ with cell dimensions a = 12.876 (3) Å, b = 14.226 (4) Å, c = 15.403 (4) Å, β = 90.54 (2)°, and Z = 2. Intensity data for I–IV were collected on a four-circle computer-controlled diffractometer with use of the θ–2θ scan technique. All four structures were solved by conventional methods, from 4550, 7167, 867, and 1964 reflections for I–IV, respectively. The structures were refined by full-matrix least-squares techniques (295 parameters for I, 357 parameters for II, 88 parameters for III, and 259 parameters for IV) to final R values of 0.046 (I), 0.062 (II), 0.049 (III), and 0.042 (IV). Complexes I and II contain the [Mo$_2$Fe$_6$S$_6$]$^{2+}$ core, and complexes III and IV contain the [Mo$_2$Fe$_6$S$_6$]$^{3+}$ core. Coordination of the Mo(CO)$_3$ units to the Fe$_6$S$_6$ central cages of I–IV results in an elongation of the latter along the $\bar{3}$ axis in III and idealized $\bar{3}$ axis in I, II, and IV. As a result of this elongation, the Fe–S bonds parallel to $\bar{3}$ axes in I–IV, in the range 2.311 (4)–2.333 (3) Å, are significantly longer than the corresponding bonds in the parent prismanes [Fe$_6$S$_6$X$_6$]$^{n-}$ (n = 3, X = Cl$^-$, Br$^-$; n = 2, X = Cl$^-$; 2.268 (8)–2.284 (3) Å). The Fe–Mo and Mo–S distances in I–IV are 3.005 (15), 2.99 (2), 2.930 (2), 2.95 (2) and 2.619 (4), 2.608 (8), 2.581 (3), 2.571 (7) Å, respectively. The electronic, cyclic voltammetric, EPR, and Mössbauer properties of the new [Fe$_6$S$_6$X$_6$(M(CO)$_3$)$_2$]$^{n-}$ adducts are discussed in detail. A comparison of these properties with the available spectroscopic data on FeMoCo of the nitrogenase enzyme is presented, and certain conclusions are drawn regarding the use of the new Fe/Mo/S adducts as a source of acceptable synthetic analogues for the nitrogenase Fe/Mo site.

Introduction

A multitude of spectroscopic techniques have been employed in the study of the heteronuclear Fe/Mo/S site in nitrogenase[2a] and the nitrogenase cofactor.[2b] In broad terms, this site is defined as a magnetically coupled (S = $^3/_2$), asymmetric aggregate[3-5] with an Fe:Mo:S ratio[6-8] of (6 ± 1):1:(7 ± 1). As indicated by extended X-ray absorption fine structure analyses (EXAFS[9-11]), structural features of this aggregate may include the FeS$_2$Mo and FeS$_2$Fe

rhombic units with Fe–Mo, Fe–S, Fe–Fe, and Mo–S distances of ~2.7, ~2.25, ~2.66, and ~2.35 Å, respectively.

In recent years, synthetic Fe/Mo/S clusters have been obtained mainly by either the spontaneous self-assembly of appropriate reagents[12,13] or by coordination of the MoS$_4$$^{2-}$ ligand to certain Fe(L)$_2$ units.[14] The heterometallic complexes thus obtained display diverse structures and, with no exception, contain the FeS$_2$Mo units. The intrinsic structural and chemical value of these compounds notwithstanding, there has been little success in obtaining synthetic Fe/Mo/S clusters that could qualify as synthetic analogues on the basis of stoichiometry. In the spontaneous self-assembly approach to synthesis, the inherent kinetic lability of the Fe/Mo/S system allows for the formation of various thermodynamically stable, heteronuclear products that, as of now, do not include one with the desired Fe:Mo:S atom ratio stated previously. Similarly, the smaller dinuclear or trinuclear MoS$_4$$^{2-}$/Fe complexes have been found rather unreactive as "building blocks" toward the stepwise synthesis of larger clusters.

Outstanding among the plethora of proposed[12] structural models for the nitrogenase active site are certain clusters that can be envisioned as derivatives of already known Fe/S compounds. One of these models[15a] (Figure 1A) contains the cubic MoFe$_7$S$_6$ core structurally analogous to that in the mineral pentlandites and the known [Co$_8$S$_6$(SPh)$_8$]$^{4-}$[15] and [Fe$_8$S$_6$(I)$_8$]$^{3-}$[16] clusters.

(1) (a) The University of Michigan. (b) Nuclear Research Center "Demokritos".
(2) (a) Orme-Johnson, W. H. *Annu. Rev. Biophys. Biophys. Chem.* **1985**, *14*, 419-459 and references therein. (b) Shah, V. K.; Brill, W. J. *Proc. Natl. Acad. Sci. U.S.A.* **1977**, *74*, 3249.
(3) Rawlings, J.; Shah, V. K.; Chisnell, J. R.; Brill, W. J.; Zimmerman, R.; Munck, E.; Orme-Johnson, W. H. *J. Biol. Chem.* **1978**, *253*, 1001.
(4) Huynh, B. H.; Munck, E.; Orme-Johnson, W. H. *Biochim. Biophys. Acta* **1979**, *527*, 192.
(5) (a) Hoffman, B. M.; Roberts, J. E.; Orme-Johnson, W. H. *J. Am. Chem. Soc.* **1982**, *104*, 860. (b) Hoffman, B. M.; Venters, R. A.; Roberts, J. E.; Nelson, M.; Orme-Johnson, W. H. *J. Am. Chem. Soc.* **1982**, *104*, 4711.
(6) (a) Burgess, B. K.; Jacogs, D. B.; Stiefel, E. I. *Biochim. Biophys. Acta* **1980**, *614*, 196. (b) Newton, W. E.; Burgess, B. K.; Stiefel, E. I. In *Molybdenum Chemistry of Biological Significance*; Newton, W. E., Otsuka, S., Eds.; Plenum: New York, 1980; p 191. (c) Burgess, B. K.; Newton, W. E. In *Nitrogen Fixation*; Mueller, A., Newton, W. E., Eds.; Plenum: New York, 1983; p 191.
(7) Nelson, M. J.; Levy, M. A.; Orme-Johnson, W. H. *Proc. Natl. Acad. Sci. U.S.A.* **1983**, *80*, 147.
(8) Orme-Johnson, W. H.; Wink, D. A.; Mclean, P. A.; Harris, G. S.; True, A. E.; Hoffman, B.; Munck, E.; Papaefthymiou, V. *Recl. Trav. Chim. Pays-Bas* **1987**, *106*, 299.
(9) (a) Cramer, S. P.; Gillum, W. D.; Hodgson, K. O.; Mortenson, L. E.; Stiefel, E. I.; Chisnell, J. R.; Brill, W. J.; Shah, V. K. *J. Am. Chem. Soc.* **1978**, *100*, 4630. (b) Cramer, S. P.; Hodgson, K. O.; Gillum, W. O.; Mortenson, L. E. *J. Am. Chem. Soc.* **1978**, *100*, 3398. (c) Conradson, S. D.; Burgess, B. K.; Newton, W. E.; Mortenson, L. E.; Hodgson, K. O. *J. Am. Chem. Soc.* **1987**, *109*, 7507 and references therein.
(10) Antonio, M. R.; Teo, B. K.; Orme-Johnson, W. H.; Nelson, M. J.; Groh, S. E.; Lindahl, P. A.; Kauzlarich, S. M.; Averill, B. A. *J. Am. Chem. Soc.* **1982**, *104*, 4703.
(11) Arber, J. M.; Flood, A. C.; Garner, C. D.; Hasnain, S. S.; Smith, B. E. *J. Phys. (Les Ulis, Fr.)* **1986**, *47*, C8-1159.
(12) Holm, R. H.; Simhon, E. D. In *Molybdenum Enzymes*; Spiro, T. G., Ed.; Wiley-Interscience: New York, 1985; Vol. 7, Chapter 1 and references therein.
(13) Christou, G.; Garner, C. D.; Mabbs, F. E.; King, T. J. *J. Chem. Soc., Chem. Commun.* **1978**, 740.
(14) Coucouvanis, D. *Acc. Chem. Res.* **1981**, *14*, 201-209 and references therein.
(15) (a) Christou, G.; Hagen, K. S.; Holm, R. H. *J. Am. Chem. Soc.* **1982**, *104*, 1744. (b) Christou, G.; Hagen, K. S.; Bashkin, J. K.; Holm, R. H. *Inorg. Chem.* **1985**, *24*, 1010.
(16) Pohl, S.; Saak, W. *Angew. Chem., Int. Ed. Engl.* **1984**, *23*, 907.
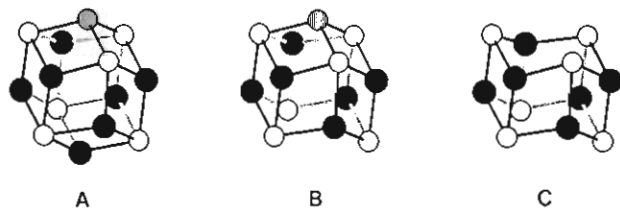
Figure 1. The rhombic dodecahedral M_8S_6 pentlandite core and topologically related fragments: (A) the hypothetical $MoFe_7S_6$ core proposed[15a] as a model for the Fe/Mo/S cluster in nitrogenase; (B) the hypothetical $MoFe_6S_6$ core; (C) the Fe_6S_6 core of the $[Fe_6S_6L_6]^{n-}$ prismanes.[17]

An entry to the synthesis of heteronuclear clusters related in core structure to the M_8S_6 pentlandite unit (Figure 1A) was suggested by the discovery of the $[Fe_6S_6Cl_6]^{2-,3-}$ clusters and derivatives.[17] The Fe_6S_6 cores in the latter (Figure 1C) are related topologically and may be convertible to the cubic M_8S_6 unit. We have demonstrated that the hexagonal Fe_3S_3 "chair" units of the Fe_6S_6 prismatic cages can serve as ligands for coordinatively unsaturated metal complexes. Recently, we have reported[18] on the synthesis and structural characterization of various $Mo(CO)_3$ and $W(CO)_3$ adducts of the $[Fe_6S_6L_6]^{3-}$ clusters that contain the new $[M_2Fe_6S_6]^{2+,3+}$ cores. In this paper, we report in detail on the synthesis and characterization of the $[Fe_6S_6X_6(Mo(CO)_3)_2]^{n-}$ clusters (M = Mo, X = Cl⁻, Br⁻, I⁻, n = 3, 4; M = W, X = Cl⁻, Br⁻, n = 3).

Experimental Section

1. General Procedures. The chemicals in this research were used as purchased. The solvents acetonitrile (CH_3CN), methylene chloride (CH_2Cl_2), 1,2-dichloroethane ($ClCH_2CH_2Cl$), and diethyl ether [($C_2H_5)_2O$] were distilled from calcium hydride (CaH_2) following refluxing under nitrogen for 12 h. Molybdenum hexacarbonyl and tungsten hexacarbonyl were purchased from Alfa. The starting materials $M(CO)_3$-$(CH_3CN)_3$ (M = Mo, W) were prepared according to procedures described in the literature.[19] Most of the synthetic work was performed under anaerobic conditions with a Vacuum Atmospheres Dri-Lab and/or vacuum-line techniques.

2. Physical Methods. Visible and ultraviolet spectra were obtained on a Cary 219 spectrophotometer using 1 mm path length quartz cuvettes. The cyclic voltammetric measurements were carried out on a PAR Model 175 universal programmer. The electrochemical cell used had platinum working and auxiliary electrodes. As reference electrode, a saturated calomel electrode was used. The solvent in the electrochemical measurements was properly dried and distilled prior to use. Tetra-*n*-butylammonium perchlorate was used as a supporting electrolyte. Normal concentrations used were 0.001 M in electroanalyte and 0.1 M in supporting electrolyte. Purified argon was used to purge the solutions prior to the electrochemical measurements.

3. Preparation of Compounds. a. Bis(tetraethylammonium) Tetrabromotetrakis(μ_3-sulfido)tetraferrate(2II,2III), [($C_2H_5)_4N]_2Fe_4S_4Br_4. A 1.00-g (4.63-mmol) sample of anhydrous $FeBr_2$, 0.92 g (6.97 mmol) of $NaSC_6H_5$, 0.49 g (2.33 mmol) of ($C_2H_5)_4NBr$, and 0.37 g (11.56 mmol)

of elemental sulfur were placed in a 125-mL Erlenmeyer flask, and to that mixture 40 mL of CH_3CN was added with continuous stirring. The resulting reaction mixture was stirred at room temperature for ca. 45 min. During that period of time, the reaction mixture became brown-green with a slight red cast. The solution was filtered to remove NaBr and unreacted elemental sulfur, and to the filtrate 100 mL of diethyl ether was added. When the solution stood for ca. 12 h, a black crystalline solid was deposited. The product was isolated by filtration, washed twice with diethyl ether, and dried under vacuum; yield 0.94 g (87.1%). The UV/visible spectrum of the crystalline product was obtained in CH_3CN and was found identical with that of the previously reported $[(C_2H_5)_4N]_2Fe_4S_4Br_4$.[20]

b. Bis(tetraethylammonium) Tetraiodotetrakis(μ_3-sulfido)tetraferrate(2II,2III), [($C_2H_5)_4N]_2Fe_4S_4I_4. A 1.00-g (3.23-mmol) sample of anhydrous FeI_2, 0.64 g (4.85 mmol) of $NaSC_6H_5$, 0.41 g (1.60 mmol) of ($C_2H_5)_4NI$, and 0.26 g (8.12 mmol) of elemental sulfur were placed in a 125-mL flask, and to that mixture 45 mL of CH_3CN was added with continuous stirring. The resulting reaction mixture was stirred at room temperature for ca. 60 min. During that period of time, the reaction mixture became deep brown-green. The solution was filtered to remove NaI and unreacted sulfur. To the filtrate was added 100–120 mL of diethyl ether, and when the mixture stood, a black crystalline solid was deposited. The product was isolated by filtration, washed twice with diethyl ether, and dried in vacuo. The crude product was recrystallized from a mixture of CH_3CN and ($C_2H_5)_2O$; yield 0.79 g (87.5%). The UV/visible spectrum of the recrystallized product was taken in CH_3CN and was found identical with that of the previously reported $[(C_2H_5)_4N]_2Fe_4S_4I_4$.[20]

c. Tetrakis(tetraethylammonium) Hexachlorohexakis(μ_4-sulfido)hexaferrate(4II,2III)–Bis(molybdenum(0) tricarbonyl), [($C_2H_5)_4N]_4Fe_6S_6Cl_6[Mo(CO)_3]_2·2CH_3CN (I). Method A. $[(C_2H_5)_4N]_3Fe_6S_6Cl_6$, 0.61 g (0.52 mmol), was dissolved in about 45 mL of CH_3CN. This solution was warmed up, and to that was added a hot solution of ~0.70 g (2.31 mmol) of $Mo(CO)_3(CH_3CN)_3$ in 10 mL of CH_3CN in three portions and with continuous stirring. The resulting mixture was stirred and heated to the boiling point for ca. 20 min. During that period of time, the reaction mixture became deep purple. The reaction mixture was allowed to cool to room temperature and was filtered, and to the filtrate was added an equal volume of diethyl ether. After 24 h of standing at ambient temperature, a black crystalline product formed and was isolated by filtration, washed twice with diethyl ether, and dried in vacuo; yield 0.26 g (58.7%).

The calculated powder pattern (2θ values (Å), $\lambda(Cu K\alpha) = 1.5418$ Å, the first 14 lines), with the relative intensities normalized to 100 (given in parentheses), is as follows: 7.716 (100.0), 8.102 (56.8), 8.617 (49.4), 9.321 (36.0), 10.725 (10.3), 11.087 (8.7), 12.339 (4.55), 13.463 (8.2), 14.867 (14.5), 16.296 (4.6), 17.489 (6.2), 18.733 (2.1), 20.782 (3.4), 21.624 (6.0). Observed: 7.70 (vs), 8.10 (s), 8.63 (s), 9.37 (m), 10.77 (w), 11.10 (w), 12.32 (vw), 13.50 (w), 14.85 (w), 16.30 (vw), 17.48 (vw), 18.70 (vw), 20.78 (vw), 21.60 (vw).

Method B. $[(C_2H_5)_4N]_2Fe_2S_2Cl_4$, 0.50 g (0.87 mmol), was dissolved in 45 mL of propionitrile. This solution was warmed up, and to that was added a hot solution of 0.70 g (2.31 mmol) of $Mo(CO)_3(CH_3CN)_3$ in 10 mL of propionitrile, in three portions and with continuous stirring. The resulting reaction mixture was stirred and heated to ~80 °C for ~30 min. The brown solution thus obtained was allowed to cool to room temperature for ca. 30 min. Subsequently, it was filtered, and to the filtrate was added an equal volume of benzene. When the solution stood at ambient temperature for 36 h, the solution deposited a black solid that was isolated, washed with diethyl ether, and dried under vacuum. Recrystallization of the crude product from $CH_3CN/(C_2H_5)_2O$ or benzene afforded a black microcrystalline product. The FTIR spectrum of the product shows the same carbonyl vibrations as those observed for the product obtained by the previous procedure (1897, 1835 cm⁻¹). Further confirmation on the identity of the product was obtained from the powder pattern and an X-ray unit cell determination of a crystal grown by diffusion of diethyl ether into an acetonitrile solution of the compound; yield 0.26 g (52.9%).

d. Tetrakis(tetraphenylphosphonium) Hexachlorohexakis(μ_4-sulfido)hexaferrate(4II,2III)–Bis(molybdenum(0) tricarbonyl), [($C_6H_5)_4P]_2Fe_6S_6Cl_6[Mo(CO)_3]_2·2CH_3CN (II). $[(C_6H_5)_4P]_2Fe_4S_4Cl_4$, 0.60 g (0.51 mmol), was dissolved in about 40 mL of CH_3CN. To this was added a hot solution of 0.23 g (0.76 mmol) of $Mo(CO)_3(CH_3CN)_3$ in 10 mL of CH_3CN, in three portions and with continuous stirring. The resulting reaction mixture was stirred and heated up for ca. 25 min. During that period of time, the reaction mixture became deep purple and did not undergo any further changes. The solution was allowed to cool to room temperature and was filtered, and to the filtrate was added an

(17) (a) Kanatzidis, M. G.; Dunham, W. R.; Hagen, W. R.; Coucouvanis, D. *J. Chem. Soc., Chem. Commun.* **1984**, 356. (b) Coucouvanis, D.; Kanatzidis, M. G.; Dunham, W. R.; Hagen, W. R. *J. Am. Chem. Soc.* **1984**, *106*, 7998. (c) Kanatzidis, M. G.; Hagen, W. R.; Dunham, W. R.; Lester, R. K.; Coucouvanis, D. *J. Am. Chem. Soc.* **1985**, *107*, 953. (d) Kanatzidis, M. G.; Salifoglou, A.; Coucouvanis, D. *J. Am. Chem. Soc.* **1985**, *107*, 3358. (e) Kanatzidis, M. G.; Salifoglou, A.; Coucouvanis, D. *Inorg. Chem.* **1986**, *25*, 2460. (f) Coucouvanis, D.; Kanatzidis, M. G.; Salifoglou, A.; Dunham, W. R.; Simopoulos, A.; Sams, J. R.; Papaefthymiou, V.; Kostikas, A.; Strouse, C. E. *J. Am. Chem. Soc.* **1987**, *109*, 6863. (g) Salifoglou, A. Ph.D. Thesis, The University of Michigan, Ann Arbor, MI.
(18) (a) Coucouvanis, D.; Kanatzidis, M. G. *J. Am. Chem. Soc.* **1985**, *107*, 5005. (b) Kanatzidis, M. G.; Coucouvanis, D. *J. Am. Chem. Soc.* **1986**, *108*, 337. (c) Salifoglou, A.; Kanatzidis, M.; Coucouvanis, D. *J. Chem. Soc., Chem. Commun.* **1986**, 559. (d) Coucouvanis, D.; Salifoglou, A.; Kanatzidis, M. G.; Simopoulos, A.; Kostikas, A. *J. Am. Chem. Soc.* **1987**, *109*, 3807.
(19) (a) Tate, D. P.; Knipple, W. R.; Augl, J. M. *Inorg. Chem.* **1962**, *1*, 433. (b) Ross, B. L.; Grasselli, J. G.; Ritchey, W. M.; Kaesz, H. D. *Inorg. Chem.* **1963**, *2*, 1023. (c) Stolz, I. W.; Dobson, G. R.; Sheline, R. K. *Inorg. Chem.* **1963**, *2*, 323.

(20) Wong, G. B.; Bobrik, M. A.; Holm, R. H. *Inorg. Chem.* **1978**, *17*, 578.

equal volume of diethyl ether. When the mixture stood for 36 h, a black microcrystalline solid was deposited, isolated by filtration, washed twice with diethyl ether, and dried under vacuum; yield 0.20 g (46.2%). The FTIR spectrum of the product was taken in the solid state (CsI pellet) and showed a doublet for the C–O stretching vibrations with frequencies that match those of the $(C_2H_5)_4N^+$ salt. The UV/visible spectrum in CH_3CN also confirmed the identity of the product as $[Fe_6S_6Cl_6(Mo-(CO)_3)_2]^{4-}$.

The calculated powder pattern (2θ values (Å), λ(Cu Kα) = 1.5418 Å, the first 14 lines), with the relative intensities normalized to 100 (given in parentheses), is as follows: 6.933 (100.0), 7.671 (32.5), 8.613 (41.2), 10.906 (30.9), 11.160 (24.2), 11.900 (14.9), 12.736 (13.6), 13.897 (12.7), 14.481 (7.8), 17.224 (8.4), 18.141 (10.4), 20.451 (11.7), 21.899 (10.9), 23.232 (7.1). Observed: 6.63 (vs), 7.65 (m), 8.48 (m), 10.43 (m), 11.30 (w), 11.70 (w), 12.70 (w), 13.85 (w), 14.73 (vw), 17.50 (vw), 18.35 (w), 20.25 (w), 21.98 (w), 23.28 (vw).

e. Tetrakis(tetraethylammonium) Hexabromohexakis(μ_4-sulfido)-hexaferrate(4II,2III)–Bis(molybdenum(0) tricarbonyl), $[(C_2H_5)_4N]_4Fe_6$-$S_6Br_6[Mo(CO)_3]_2$. This compound was obtained by a procedure identical with the one described for the synthesis of $(Ph_4P)_4[Fe_6S_6Cl_6(Mo(CO)_3)_2]$ in the reaction of $(Et_4N)_2Fe_4S_4Br_4$ (0.92 g, 0.99 mmol) with Mo(C-O)$_3$(CH$_3$CN)$_3$ (0.60 g, 1.98 mmol) in 40 mL of CH_3CN solution. The yield was 0.32 g (51.5%).

The observed powder pattern (2θ values (Å), λ(Cu Kα) = 1.5418 Å, the first 14 lines) is as follows: 7.60 (m), 8.33 (vs), 8.83 (s), 10.60 (vw), 11.90 (vw), 13.05 (vw), 14.25 (vw), 15.40 (vw), 16.58 (vw), 17.80 (w), 18.95 (vw), 20.15 (vw), 21.38 (w), 23.10 (vw). Anal. Calcd for Mo$_2$-Fe$_6$S$_6$Br$_6$N$_4$O$_6$C$_{38}$H$_{80}$ (M_r = 1888): Fe, 17.80; Mo, 10.17. Found: Fe, 19.58; Mo, 10.18.

f. Tetrakis(tetraphenylphosphonium) Hexaiodohexakis(μ_4-sulfido)-hexaferrate(4II,2III)–Bis(molybdenum(0) tricarbonyl), $[(C_6H_5)_4P]_4Fe_6$-$S_6I_6[Mo(CO)_3]_2$. $[(C_6H_5)_4P]_4Fe_6S_6Cl_6[Mo(CO)_3]_2$, 0.40 g (0.16 mmol), was dissolved in about 40–45 mL of acetonitrile. To this solution was added 0.14 g (0.93 mmol) of NaI solid, with continuous stirring. The resulting reaction mixture was then stirred for ca. 15–20 min. During that period of time, the reaction mixture became deep brown with a slight greenish cast. The reaction mixture was filtered to remove NaCl, and to the filtrate was added an equal volume of anhydrous ether. After 24 h, a black microcrystalline solid precipitated out of solution. The product was isolated by filtration, washed with two 10-mL portions of diethyl ether, and dried in vacuo; yield 0.34 g (71.8%). Anal. Calcd for Mo$_2$-Fe$_6$S$_6$I$_6$P$_4$O$_6$C$_{102}$H$_{80}$ (M_r = 3006): Fe, 11.18; Mo, 6.38. Found: Fe, 11.18; Mo, 6.07.

g. Tetrakis(tetraethylammonium) Hexaiodohexakis(μ_4-sulfido)hexa-ferrate(4II,2III)–Bis(molybdenum(0) tricarbonyl), $[(C_2H_5)_4N]_4Fe_6S_6I_6$-$[Mo(CO)_3]_2$. This compound was obtained by a procedure identical with the one described for the synthesis of the bromo analogue in the reaction of $(Et_4N)_2Fe_4S_4I_4$ (1.14 g, 1.02 mmol) with Mo(CO)$_3$(CH$_3$CN)$_3$ in 50 mL of CH_3CN; yield 0.56 g (76.1%). The UV/visible spectrum of the product was obtained in acetonitrile and showed a band at 360 nm. The solution FTIR spectrum of the product (in CH_3CN) shows a doublet for the carbonyl ligands with frequencies at 1917 and 1857 cm^{-1}, very close to those observed for the $[(C_6H_5)_4P]^+$ salt of $[Fe_6S_6I_6(Mo(CO)_3)_2]^{4-}$.

h. Tris(tetraethylammonium) Hexachlorohexakis(μ_4-sulfido)hexa-ferrate(3II,3III)–Bis(molybdenum(0) tricarbonyl), $[(C_2H_5)_4N]_3Fe_6S_6$-Cl$_6[Mo(CO)_3]_2$ (III). Method A. $[(C_2H_5)_4N]_3Fe_6S_6Cl_6$, 0.60 g (0.51 mmol), was suspended in 40–45 mL of 1,2-dichloroethane, ClCH$_2$CH$_2$Cl, and the heterogeneous solution was warmed up. To that was added a hot solution of 0.62 g (2.05 mmol) of Mo(CO)$_3$(CH$_3$CN)$_3$ in 20 mL of ClCH$_2$CH$_2$Cl, in three portions and with continuous stirring. The resulting slurry was stirred and heated up to boiling for ca. 60 min. During that period of time, the reaction mixture became dark brown. The reaction mixture was allowed to cool to room temperature over a period of 2–3 h, at which time the crude product had precipitated out of solution, leaving a slightly brown supernatant liquid. The crude product was isolated by filtration, washed with diethyl ether, and dried in vacuo. This crude product was then recrystallized from a warm CH_3CN/diethyl ether mixture, affording a pure black microcrystalline material; yield 0.46 g (60.3%). The powder pattern of the recrystallized material was obtained and is almost identical with that calculated on the basis of the single-crystal X-ray crystallographic atomic coordinates (rhombohedral phase).

The calculated powder pattern (2θ values (Å), λ(Cu Kα) = 1.5418 Å, the first 13 lines), with the relative intensities normalized to 100 (given in parentheses), is as follows: 8.661 (100.0), 9.156 (53.1), 12.615 (12.0), 13.798 (1.9), 15.013 (18.1), 18.405 (4.7), 20.899 (4.0), 21.511 (5.0), 23.820 (7.6), 25.405 (4.7), 26.886 (9.9), 27.745 (3.1), 28.337 (3.5). Observed: 8.55 (vs), 9.30 (s), 12.65 (w), 13.80 (vw), 15.00 (w), 18.35 (vw), 20.90 (vw), 21.55 (vw), 23.85 (vw), 25.45 (vw), 26.88 (w), 27.78 (vw), 28.40 (vw).

Method B. $[(C_2H_5)_4N]_3Fe_6S_6(OC_6H_4$-$p$-$CH_3)_6[Mo(CO)_3]_2$ (0.50 g, 0.26 mmol) was dissolved in about 45 mL of CH_3CN. To that solution

was added a solution of 0.22 g (1.56 mmol, 0.182 mL) of C$_6$H$_5$COCl in 10 mL of CH_3CN, dropwise with continuous stirring over a period of 5–8 min. The resulting reaction mixture was stirred at room temperature for ca. 30 min. During that period of time, the reaction mixture gradually changed to deep purple. The reaction mixture was filtered, and to the filtrate was added an equal volume of diethyl ether. When the mixture stood overnight, a black microcrystalline solid was deposited. This was isolated by filtration, washed with two 10-mL portions of diethyl ether, and dried in vacuo; yield 0.30 g (77.3%). The UV/visible spectrum of the product taken in CH_3CN (λ_{max} = 460 nm), the FTIR spectrum (CsI pellet; 1925 cm^{-1}), and the X-ray powder pattern confirmed the identity of the compound as $[(C_2H_5)_4N]_3Fe_6S_6Cl_6[Mo(CO)_3]_2$.

i. Tris(tetraphenylphosphonium) Hexachlorohexakis(μ_4-sulfido)-hexaferrate(3II,3III)–Bis(molybdenum(0) tricarbonyl), $[(C_6H_5)_4P]_3Fe_6$-$S_6Cl_6[Mo(CO)_3]_2$. Method A. $[(C_6H_5)_4P]_4Fe_6S_6Cl_6[Mo(CO)_3]_2$, 0.17 g (0.07 mmol), was suspended in 40 mL of methylene chloride. To this suspension was added a solution of 0.03 g (0.09 mmol) of $(C_5H_5)_2FePF_6$ in ~10 mL of CH$_2$Cl$_2$, dropwise with continuous stirring over a period of 8 min. The resulting reaction mixture was stirred for ca. 4 h. During that period of time, all of the starting material went into solution and the reaction mixture became purple. The solution was filtered, and to the filtrate was added an equal volume of diethyl ether. When the mixture stood overnight, a black crystalline product was deposited, isolated by filtration, washed twice with diethyl ether, and dried in vacuo; yield 0.12 g (84.6%).

The solution FTIR spectrum of the product (CH_3CN) shows C=O vibrational frequencies identical with those found for the $(C_2H_5)_4N^+$ salt. The UV/visible spectrum of the product was obtained in CH_3CN and is the same as that of the $(C_2H_5)_4N^+$ salt. The above confirmed the identity of the product as $Fe_6S_6Cl_6[Mo(CO)_3]_2^{3-}$.

Method B. $[(C_6H_5)_4P]_2Fe_6S_6Cl_6$, 0.97 g (0.68 mmol), was dissolved in ~50 mL of 1,2-dichloroethane. The solution was gently warmed up, and to that was added a hot solution of 0.83 g (2.74 mmol) of Mo(C-O)$_3$(CH$_3$CN)$_3$ in 10 mL of ClCH$_2$CH$_2$Cl, in three portions and with continuous stirring. The resulting reaction mixture was stirred and heated up to boiling for 20–30 min. During that period of time, the reaction mixture became purple. The reaction mixture was allowed to cool to room temperature and was filtered, and to the filtrate was added an equal volume of diethyl ether. When the mixture stood for ca. 12 h, a brown-black microcrystalline solid was deposited. The product was isolated by filtration, washed with two 5-mL portions of diethyl ether, and dried under vacuum; yield 0.50 g (69.1%). The product can be recrystallized from mixtures of CH$_2$Cl$_2$/(C$_2$H$_5$)$_2$O or ClCH$_2$CH$_2$Cl/(C$_2$H$_5$)$_2$O. The UV/visible spectrum of the product was taken in CH_3CN and was identical with that of the product prepared by method A. The solution FTIR spectrum (CH$_3$CN) was also identical with that obtained in method A. These data confirm the identity of the product as $Fe_6S_6Cl_6[Mo(CO)_3]_2^{3-}$.

j. Tris(tetraethylammonium) Hexabromohexakis(μ_4-sulfido)hexa-ferrate(3II,3III)–Bis(molybdenum(0) tricarbonyl) (A), $[(C_2H_5)_4N]_3Fe_6$-$S_6Br_6[Mo(CO)_3]_2$ (IV). This compound was obtained by a procedure identical with the one described for the synthesis of the Ph$_4$P$^+$ salt of the analogous chloro complex by the oxidation of $(Et_4N)_4[Fe_6S_6Br_6(Mo-(CO)_3)_2]$ (0.30 g, 0.16 mmol) with $[(Cp)_2Fe]PF_6$ (0.06 g, 0.17 mmol) in 40 mL of CH_3CN.

The X-ray powder pattern of the crystalline material was obtained and found very similar to that of the rhombohedral $[(C_2H_5)_4N]_3Fe_6S_6Cl_6$-$[Mo(CO)_3]_2$ analogue. The FTIR spectrum of the crystalline product was taken, and it showed the C–O stretching vibrations having a frequency identical with that of the chloro analogue. The compound can also be prepared in 48% yield by the reaction of $[(C_2H_5)_4N]_3Fe_6S_6$-$(OC_6H_4$-p-$CH_3)_6[Mo(CO)_3]_2$ with C$_6$H$_5$COBr in CH_3CN in a 1:6 molar ratio. This procedure is identical with the one employed for the synthesis of the analogous chloro compound.

k. Tris(tetraethylammonium) Hexabromohexakis(μ_4-sulfido)hexa-ferrate(3II,3III)–Bis(molybdenum(0) tricarbonyl) (B), $[(C_2H_5)_4N]_3Fe_6$-$S_6Br_6[Mo(CO)_3]_2$. $[(C_2H_5)_4N]_4Fe_6S_6Br_6[Mo(CO)_3]_2$, 0.34 g (0.18 mmol), was dissolved in ~40 mL of CH_3CN. To that solution was added a solution of 0.09 g (0.27 mmol) of $[(C_5H_5)_2]FePF_6$ in 10 mL of CH_3CN, dropwise with a Pasteur pipet with continuous stirring over a period of 5–8 min. The resulting reaction mixture was stirred at room temperature for ca. 40 min. During that period of time, the reaction mixture became brown with a purple cast. The solution was filtered, and to the filtrate was added an equal volume of diethyl ether. The microcrystalline solid that was deposited upon standing for ~12 h was isolated by filtration, washed with diethyl ether, and dried under vacuum; yield 0.20 g (63.2%). The solution FTIR spectrum of the isolated product was taken in CH_3CN and came out to be identical with that of the rhombohedral phase of the analogous chloro complex. The powder pattern of this compound was different from that of the rhombohedral chloro analogue. Further documentation of this formulation was furnished by single-crystal X-ray

Table I. Summary of Crystal Data, Intensity Collection, and Structure Refinement Data for $(Et_4N)_4Fe_6S_6Cl_6[Mo(CO)_3]_2\cdot2CH_3CN$ (I), $(Ph_4P)_4Fe_6S_6Cl_6(Mo(CO)_3)_2\cdot2CH_3CN$ (II), $[(C_2H_5)_4N]_3Fe_6S_6Cl_6[Mo(CO)_3]_2$ (III), and $[(C_2H_5)_4N]_3Fe_6S_6Br_6[Mo(CO)_3]_2$ (IV)

	$Mo_2Fe_6S_6Cl_6O_6N_6$- $C_{42}H_{86}$	$Mo_2Fe_6S_6Cl_6O_6P_4N_2$- $C_{106}H_{86}$	$Mo_2Fe_6S_6Cl_6O_6N_3$- $C_{30}H_{60}$	$Mo_2Fe_6S_6Br_6O_6N_3$- $C_{30}H_{60}$
mol wt	1703	2539	1491	1758
a, Å	13.192 (2)	16.329 (6)	14.073 (2)	12.876 (3)
b, Å	16.504 (5)	16.253 (6)	14.073 (2)	14.226 (4)
c, Å	16.080 (4)	20.588 (5)	14.073 (2)	15.403 (4)
α, deg	90.00	90.00	93.11 (1)	90.00
β, deg	97.97 (2)	94.97 (3)	93.11 (1)	90.54 (2)
γ, deg	90.00	90.00	93.11 (1)	90.00
V, Å³; Z	3467 (1); 2	5443 (3); 2	2774 (1); 2	2821 (1); 2
d_{calc}, g/cm³	1.64	1.54	1.78	2.07
d_{obs}, g/cm³ ^{a}	1.63	1.55	1.74	2.07
space group	$P2_1/n$	$P2_1/n$	$R\bar{3}c$	$P2_1/n$
cryst dimens, mm	0.30 × 0.42 × 0.28	0.55 × 0.29 × 0.11	0.09 × 0.14 × 0.10	0.12 × 0.14 × 0.15
abs coeff (μ), cm⁻¹	19.69	13.20	24.53	63.18
radiation ($\lambda_{K\alpha}$, Å)	Mo Kα (0.71069)	Mo Kα (0.71069)	MoKα (0.71069)	Mo Kα (0.71069)
$2\theta_{max}$, deg	45	45	40	40
no. of data collected;^{b} octants	4992; $h,k,\pm l$	7789; $h,\pm k,\pm l$	5513; $h,\pm k,\pm l$	2757; $h,k,\pm l$
scan speed, min − max, deg/min	3.0, 29.3	3.0, 29.3	2.9, 29.3	2.9, 29.3
no. of unique data	4550	7167	867	1964
no. of data used in refinement, $F_o^2 > 3\sigma(F_o^2)$	3286	5128	664	1737
no. of atoms in asymmetric unit	65	112	19.83	59.5
no. of variables	295	357	88	259
phasing technique	direct methods	direct methods	direct methods	direct methods
R, %^{c}	4.39	6.18	4.93	4.21
R_w, %^{c}	4.45	6.14	5.03	3.92

^{a} By flotation in $CCl_4/CHBr_3$/pentane mixture. ^{b} At ambient temperature. $^c R = \sum||F_o| - |F_c||/\sum|F_o|$; $R_w = [\sum w(|F_o| - |F_c|)^2/\sum w|F_o|^2]^{1/2}$.

crystallographic work, which showed the same anion but in a monoclinic phase.

The calculated powder pattern (2θ values (Å), λ(Cu Kα) = 1.5418 Å, the first 12 lines), with the relative intensities normalized to 100 (given in parentheses), is as follows: 8.475 (100.0), 8.965 (84.3), 9.213 (80.5), 11.490 (4.4), 12.443 (2.9), 13.745 (2.5), 14.810 (15.1), 16.189 (3.5), 18.563 (9.7), 19.558 (26.8), 20.785 (6.8), 21.531 (8.1). Observed: 8.45 (vs), 9.00 (s), 9.25 (s), 11.45 (vw), 12.60 (vw), 13.73 (vw), 14.83 (w), 16.15 (vw), 18.60 (vw), 19.58 (m), 20.75 (vw), 21.50 (vw).

l. Tris(tetraphenylphosphonium) Hexaiodohexakis(μ_4-sulfido)hexaferrate(3II,3III)–Bis(molybdenum(0) tricarbonyl), $[(C_6H_5)_4P]_3Fe_6S_6I_6$[Mo(CO)$_3$]$_2$. Method A. This compound was obtained by a procedure identical with the one described for the synthesis of $[Ph_4P]_4Fe_6S_6I_6$[Mo(CO)$_3$]$_2$ by a metathetical reaction between $(Ph_4P)_3Fe_6S_6Cl_6$[Mo(CO)$_3$]$_2$ (0.66 g, 0.31 mmol) and NaI (0.28 g, 1.87 mmol) in 45 mL of CH_3CN; yield 0.54 g (~65%). The UV/visible spectrum of the product was taken in CH_3CN and showed a band at 380 nm and a shoulder around 420 nm (sh). The FTIR spectrum (CsI pellet) was also obtained and shows a sharp doublet for the carbonyl ligands with frequencies at 1936 and 1904 cm⁻¹.

The observed powder pattern (2θ values (Å), λ(Cu Kα) = 1.5418 Å, the first 15 lines) is as follows: 7.00 (s), 7.78 (vs), 9.98 (vw), 10.90 (vw), 11.85 (vw), 12.58 (vw), 13.50 (vw), 14.60 (m), 16.28 (vw), 16.90 (vw), 20.03 (vw), 20.75 (s), 23.30 (m), 25.48 (w), 27.20 (vw). Anal. Calcd for $Mo_2Fe_6S_6I_6P_3O_6C_{78}H_{60}$ (M_r = 2667): Fe, 12.60; Mo, 7.20. Found: Fe, 11.18; Mo, 5.99.

Method B. This complex can also be obtained in ~88% yield by the oxidation of $[Ph_4P]_4Fe_6S_6I_6$[Mo(CO)$_3$]$_2$ with $[(Cp)_2Fe]PF_6$ in CH_2Cl_2, as described for the synthesis of the analogous chloro complex.

m. Tris(tetraethylammonium) Hexachlorohexakis(μ_4-sulfido)hexaferrate(3II,3III)–Bis(tungsten(0) tricarbonyl), $[(C_2H_5)_4N]_3Fe_6S_6Cl_6$[W(CO)$_3$]$_2$. $[(C_2H_5)_4N]_3Fe_6S_6(OC_6H_4\text{-}p\text{-}CH_3)_6$[W(CO)$_3$]$_2$, 0.51 g (0.24 mmol), was dissolved in ~40 mL of CH_3CN. To that was added a solution of ~0.21 g (1.46 mmol, 0.169 mL) of C_6H_5COCl in 10 mL of CH_3CN, dropwise with a Pasteur pipet with continuous stirring over a period of ~8 min. The resulting reaction mixture was stirred at room temperature for ca. 45 min, and the reaction mixture became purple with a brown cast. The reaction mixture was filtered, and to the filtrate was added an equal volume of diethyl ether. When the mixture stood, a microcrystalline solid formed and was isolated by filtration, washed twice with diethyl ether, and dried under vacuum; yield 0.18 g (44.4%). The X-ray powder pattern of the product was obtained and compared with that of the Mo analogue. The two powder patterns were identical, thus confirming the identity of the isolated compound as $[(C_2H_5)_4N]_3Fe_6S_6Cl_6$[W(CO)$_3$]$_2$.

**n. Tris(tetraethylammonium) Hexabromohexakis(μ_4-sulfido)hexaferrate(3II,3III)–Bis(tungsten(0) tricarbonyl), $[(C_2H_5)_4N]_3Fe_6S_6Br_6$-

$[W(CO)_3]_2$.** This compound can be obtained by a procedure identical with the one described for the synthesis of the chloro analogue, using C_6H_5COBr; yield 0.09 g (42.4%). The X-ray powder pattern of the product was obtained and was very similar to that of the Mo analogue.

4. X-ray Diffraction Measurements. a. Collection of Data. Single crystals of $[(C_2H_5)_4N]_4Fe_6S_6Cl_6[Mo(CO)_3]_2\cdot2CH_3CN$ (I), $[(C_6H_5)_4P]_4Fe_6S_6Cl_6[Mo(CO)_3]_2\cdot2CH_3CN$ (II), $[(C_2H_5)_4N]_3Fe_6S_6Cl_6[Mo(CO)_3]_2$ (III), and $[(C_2H_5)_4N]_3Fe_6S_6Br_6[Mo(CO)_3]_2$ (IV) were obtained by the slow diffusion of diethyl ether into CH_3CN solutions of the complexes. Crystal and refinement data for I–IV are compiled in Table I. The single crystals obtained for I–IV had the shapes of flat hexagonal plates, rectangular prisms, oblique quadrangular prisms, and rectangular prisms, respectively. A single crystal for each complex was carefully chosen and mounted in a thin-walled, sealed capillary tube. Diffraction data were collected on a Nicolet P3/F four-circle computer-controlled diffractometer at ambient temperature, for all complexes. A detailed description of the instrument and the data acquisition procedures have been described previously.[21]

Intensity data for II and III were collected on half of the reciprocal lattice sphere. Intensity data for I and IV were collected on one-fourth of the reciprocal lattice sphere (Table I).

Preliminary unit cell parameters for all complexes were determined by using 15 well-centered reflections whose x and y coordinates were obtained from a random orientation photograph.

Accurate cell parameters were obtained from a least-squares fit of the angular settings of 25 machine-centered reflections with 2θ values between 25 and 40°.

Details concerning crystal characteristics and X-ray diffraction methodology are given in Table I.

b. Reduction of Data. The raw data were reduced to net intensities, estimated standard deviations were calculated on the basis of counting statistics, Lorentz–polarization corrections were applied, and equivalent reflections were averaged. The estimated standard deviation of the structure factor was taken as the larger of that derived from counting statistics and that derived from the scatter of multiple measurements.

The least-squares program used minimizes $\sum w(\Delta|F|)^2$. The weighting function used throughout the refinement of the structures gives zero weight to those reflections with $F^2 \leq 3\sigma(F^2)$ and $w = 1/\sigma^2(F)$ to all others.[22]

For the intensity data of $[Fe_6S_6Br_6(Mo(CO)_3)_2]^{3-}$, an analytical absorption correction was applied using the ABSC instruction in the SHELX76 package. The minimum and maximum absorption corrections were 0.396 and 0.527, respectively.

(21) Kanatzidis, M. G.; Coucouvanis, D. *Inorg. Chem.* **1984**, *23*, 4192.
(22) Grant, D. F.; Killean, R. C. G.; Lawrence, J. L. *Acta Crystallogr.* **1969**, *B25*, 374.

Table II. Fractional Atomic Coordinates[a,b] and Equivalent Isotropic Thermal Parameters for the Non-Hydrogen Atoms in $[(C_2H_5)_4N]_4Fe_6S_6Cl_6[Mo(CO)_3]_2\cdot 2CH_3CN$ (I)

atom	x	y	z	U
Mo1	0.4368 (01)	0.1440 (00)	0.0832 (00)	0.0442
Fe1	0.3250 (01)	−0.0003 (01)	0.0061 (01)	0.0435
Fe2	0.5373 (01)	0.1185 (01)	−0.0733 (01)	0.0422
Fe3	0.5845 (01)	0.0094 (01)	0.1370 (01)	0.0422
S1	0.6255 (02)	0.1169 (01)	0.0592 (01)	0.0439
S2	0.4119 (02)	−0.0026 (01)	0.1394 (01)	0.0438
S3	0.3645 (02)	0.1079 (01)	−0.0728 (01)	0.0434
Cl1	0.1551 (02)	−0.0104 (02)	0.0048 (02)	0.0708
Cl2	0.5805 (02)	0.2270 (01)	−0.1452 (02)	0.0638
Cl3	0.6780 (02)	0.0189 (02)	0.2643 (01)	0.0695
CX1	0.3003 (08)	0.1762 (06)	0.1051 (06)	0.0668
CX2	0.4534 (07)	0.2581 (06)	0.0516 (06)	0.0567
CX3	0.4782 (08)	0.1754 (06)	0.1998 (06)	0.0616
O1	0.2215 (06)	0.1981 (05)	0.1188 (05)	0.0971
O2	0.4618 (06)	0.3257 (04)	0.0358 (05)	0.0801
O3	0.4982 (06)	0.1959 (05)	0.2697 (05)	0.0932
N1	0.9253 (06)	0.0249 (04)	0.7379 (04)	0.0555
C4	0.8639 (08)	0.1019 (06)	0.7186 (07)	0.0691
C5	0.8149 (10)	0.1340 (07)	0.7911 (08)	0.1091
C6	1.0088 (08)	0.0360 (06)	0.8118 (07)	0.0721
C7	1.0851 (09)	0.1015 (07)	0.7990 (07)	0.0895
C8	0.9654 (08)	0.0076 (06)	0.6556 (07)	0.0758
C9	1.0324 (10)	−0.0656 (07)	0.6582 (08)	0.1078
C10	0.8612 (08)	−0.0439 (06)	0.7617 (06)	0.0179
C11	0.7718 (08)	−0.0673 (07)	0.6978 (07)	0.0873
N2	0.3767 (08)	0.1958 (05)	0.5882 (06)	0.0877
C12	0.4355 (23)	0.1242 (19)	0.5588 (20)	0.0752
C13	0.4353 (26)	0.1320 (22)	0.4666 (23)	0.1576
C12′	0.4390 (27)	0.1178 (21)	0.5871 (21)	0.0896
C13′	0.5388 (17)	0.1081 (13)	0.6384 (14)	0.0783
C14	0.3837 (29)	0.2754 (22)	0.5485 (23)	0.1442
C15	0.4835 (20)	0.2765 (17)	0.4974 (17)	0.1003
C14′	0.4517 (27)	0.2771 (20)	0.5949 (20)	0.0994
C15′	0.4869 (34)	0.2921 (27)	0.5698 (31)	0.1563
C16	0.3644 (10)	0.1915 (08)	0.6772 (08)	0.1016
C17	0.2973 (10)	0.2555 (08)	0.7083 (09)	0.1226
C18	0.2543 (22)	0.1818 (18)	0.5339 (16)	0.0737
C19	0.2078 (21)	0.1063 (17)	0.5534 (16)	0.0828
C18′	0.2885 (20)	0.2092 (15)	0.5303 (15)	0.0680
C19′	0.2100 (25)	0.1467 (21)	0.5458 (19)	0.0976
N3	0.7118 (11)	0.0700 (09)	0.5151 (09)	0.1584
CS1	0.7242 (10)	0.1852 (07)	0.4104 (08)	0.0972
CS2	0.7163 (11)	0.1221 (09)	0.4684 (10)	0.1136

[a] Calculated standard deviations are indicated in parentheses. [b] The equivalent isotropic thermal parameters are in units of square angstroms.

The refinement calculations were carried out on the University of Michigan Amdahl 800 computer using the locally adapted SHELX76 crystallographic program package.

c. Determination of Structures. $[(C_2H_5)_4N]_4Fe_6S_6Cl_6[Mo(CO)_3]_2\cdot 2C-H_3CN$ (I). The structure was solved by the direct-methods routine SOLV of the SHELXTL84 crystallographic program package. In the space group $P2_1/n$ with $Z = 2$, the $[Fe_6S_6Cl_6(Mo(CO)_3)_2]^{4-}$ anion is required by symmetry to reside on a crystallographic inversion center. The positions of the molybdenum and the three iron atoms were located around $^1/_2$, 0, 0. Subsequent difference Fourier and electron density maps revealed the three sulfur and three chlorine atoms of the $[MoFe_3S_3Cl_3]$ fragment in the asymmetric unit. The remaining non-hydrogen atoms in the anion and the two tetraethylammonium cations were located through successive electron density difference Fourier maps following least-squares refinements of the input atomic coordinates. Refinement of all the atoms in the asymmetric unit with isotropic temperature factors led to a conventional R value of 0.11. The two tetraethylammonium cations reside in general positions. In one of the cations, three of the four ethyl groups were found to be positionally disordered in two orientations relative to the pseudo-3-fold axis that passes through the N atom and fourth ethyl group. Refinement was successful with the carbon atoms in the disordered ethyl groups assigned 0.50 occupancy factors. The CH_3CN molecule of solvation also was located in a general position and was included in the refinement. The refinement process then continued with full-matrix least-squares techniques following the assignment of anisotropic temperature factors to all non-hydrogen atoms in the asymmetric unit that were not subject to disorder. The refinement converged to an R value of 0.057. At this stage, the hydrogen atom positions for all

Table III. Fractional Atomic Coordinates[a,b] and Equivalent Isotropic Thermal Parameters for the Non-Hydrogen Atoms in $[(C_6H_5)_4P]_4Fe_6S_6Cl_6[Mo(CO)_3]_2\cdot 2CH_3CN$ (II)

atom	x	y	z	U
Mo1	0.1612 (01)	0.9926 (01)	−0.0479 (00)	0.0483
Fe1	0.1016 (01)	1.0393 (01)	0.0778 (01)	0.0367
Fe2	0.0063 (01)	1.0859 (01)	−0.0915 (01)	0.0425
Fe3	0.0298 (01)	0.8658 (01)	−0.0324 (01)	0.0428
S1	0.0266 (01)	0.9526 (02)	−0.1196 (01)	0.0444
S2	0.1231 (01)	0.9046 (02)	0.0511 (01)	0.0448
S3	0.0985 (01)	1.1285 (02)	−0.0083 (01)	0.0470
Cl1	0.1961 (01)	1.0796 (02)	0.1586 (01)	0.0525
Cl2	−0.0028 (02)	1.1622 (02)	−0.1838 (01)	0.0725
Cl3	0.0412 (02)	0.7355 (02)	−0.0654 (02)	0.0922
CX1	0.2675 (06)	1.0141 (06)	0.0010 (05)	0.0552
CX2	0.2057 (06)	1.0584 (10)	−0.1153 (05)	0.0995
CX3	0.2125 (07)	0.9013 (09)	−0.0880 (06)	0.0902
O1	0.3319 (04)	1.0268 (05)	0.0288 (04)	0.0801
O2	0.2383 (06)	1.0976 (08)	−0.1529 (04)	0.1488
O3	0.2443 (05)	0.8448 (07)	−0.1111 (05)	0.1389
P1	0.7698 (01)	0.5190 (01)	0.0229 (01)	0.0411
P2	0.4684 (01)	0.8854 (01)	0.1771 (01)	0.0430
C1	0.7686 (06)	0.4521 (05)	−0.0464 (04)	0.0395
C2	0.7490 (06)	0.4851 (06)	−0.1093 (04)	0.0489
C3	0.7499 (06)	0.4339 (06)	−0.1633 (05)	0.0579
C4	0.7701 (06)	0.3521 (07)	−0.1557 (05)	0.0640
C5	0.7902 (06)	0.3204 (06)	−0.0952 (05)	0.0611
C6	0.7889 (06)	0.3701 (06)	−0.0392 (05)	0.0495
C7	0.7146 (06)	0.4708 (06)	0.0836 (04)	0.0485
C8	0.6485 (07)	0.4233 (07)	0.0679 (05)	0.0692
C9	0.6024 (08)	0.3902 (08)	0.1175 (07)	0.0921
C10	0.6264 (08)	0.4090 (09)	0.1800 (07)	0.0936
C11	0.6905 (09)	0.4576 (09)	0.1968 (07)	0.1002
C12	0.7382 (07)	0.4892 (07)	0.1490 (06)	0.0722
C13	0.7207 (05)	0.6139 (05)	0.0005 (04)	0.0394
C14	0.7636 (06)	0.6761 (06)	−0.0285 (05)	0.0505
C15	0.7243 (06)	0.7497 (06)	−0.0468 (05)	0.0558
C16	0.6422 (07)	0.7586 (07)	−0.0383 (05)	0.0672
C17	0.5984 (07)	0.6967 (07)	−0.0105 (05)	0.0644
C18	0.6392 (06)	0.6245 (06)	0.0087 (05)	0.0564
C19	0.8727 (05)	0.5383 (05)	0.0578 (04)	0.0412
C20	0.9284 (06)	0.4742 (06)	0.0625 (05)	0.0524
C21	1.0057 (07)	0.4850 (07)	0.0955 (05)	0.0630
C22	1.0251 (07)	0.5595 (07)	0.1219 (05)	0.0702
C23	0.9740 (07)	0.6229 (07)	0.1169 (06)	0.0748
C24	0.8952 (06)	0.6145 (06)	0.0856 (05)	0.0614
C25	0.3805 (05)	0.8574 (06)	0.2184 (04)	0.0439
C26	0.3029 (06)	0.8863 (06)	0.1945 (05)	0.0555
C27	0.2343 (06)	0.8674 (07)	0.2277 (05)	0.0634
C28	0.2449 (06)	0.8209 (06)	0.2833 (05)	0.0608
C29	0.3194 (06)	0.7936 (06)	0.3065 (05)	0.0613
C30	0.3889 (06)	0.8109 (06)	0.2756 (05)	0.0554
C31	0.5559 (06)	0.8251 (06)	0.2055 (05)	0.0520
C32	0.5921 (07)	0.8362 (07)	0.2694 (05)	0.0702
C33	0.6590 (08)	0.7875 (08)	0.2898 (07)	0.0954
C34	0.6888 (09)	0.7333 (10)	0.2481 (08)	0.1159
C35	0.6535 (09)	0.7202 (09)	0.1861 (08)	0.1107
C36	0.5860 (07)	0.7681 (07)	0.1642 (06)	0.0759
C37	0.4461 (05)	0.8647 (05)	0.0918 (04)	0.0417
C38	0.4922 (05)	0.9043 (06)	0.0469 (04)	0.0448
C39	0.4769 (06)	0.8859 (06)	−0.0181 (04)	0.0487
C40	0.4171 (06)	0.8299 (06)	−0.0391 (05)	0.0606
C41	0.3735 (07)	0.7905 (07)	0.0054 (05)	0.0672
C42	0.3867 (06)	0.8079 (06)	0.0717 (05)	0.0577
C43	0.4938 (06)	0.9926 (06)	0.1911 (05)	0.0454
C44	0.4314 (07)	1.0487 (07)	0.1944 (05)	0.0649
C45	0.4522 (07)	1.1335 (07)	0.2051 (06)	0.0762
C46	0.5318 (08)	1.1551 (08)	0.2122 (06)	0.0787
C47	0.5927 (07)	1.1006 (08)	0.2079 (06)	0.0767
C48	0.5749 (06)	1.0170 (06)	0.1973 (05)	0.0604
N1	0.4619 (07)	0.5889 (08)	0.0902 (07)	0.1179
CS1	0.4643 (10)	0.5810 (10)	0.1421 (09)	0.1172
CS2	0.4692 (10)	0.5686 (11)	0.2139 (08)	0.1351

[a] Calculated standard deviations are indicated in parentheses. [b] The equivalent isotropic thermal parameters are in units of square angstroms.

nondisordered carbon atoms were calculated. In the final refinement, they were included in the structure factor calculation at 0.95 Å from the
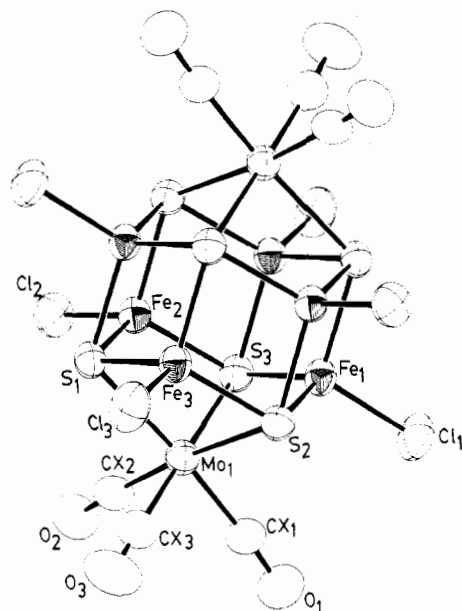
Figure 2. Structure and labeling of the $[Fe_6S_6X_6(Mo(CO)_3)_2]^{n-}$ anions in I and II ($n = 4$, $X = Cl^-$), III ($n = 3$, $X = Cl^-$), and IV ($n = 3$, $X = Br^-$). Thermal ellipsoids as drawn by ORTEP represent the 50% probability surfaces.

Table IV. Fractional Atomic Coordinates[a,b] and Equivalent Isotropic Thermal Parameters for the Non-Hydrogen Atoms in $[(C_2H_5)_4N]_3Fe_6S_6Cl_6[Mo(CO)_3]_2$ (III)

atom	x	y	z	U
Mo1	−0.1219 (01)	−0.1219 (01)	−0.1219 (01)	0.0525
Fe1	0.0012 (01)	−0.1563 (01)	0.0459 (01)	0.0427
S1	−0.1025 (02)	0.0582 (02)	−0.1478 (02)	0.0431
Cl1	0.0036 (02)	−0.3030 (02)	0.0974 (03)	0.0618
CX1	−0.1363 (11)	−0.2657 (12)	−0.1271 (11)	0.0738
O1	−0.1433 (09)	−0.3472 (08)	−0.1316 (09)	0.0982
N1	−0.4391 (08)	0.9390 (08)	0.2500 (-)	0.0603
C1	−0.4618 (22)	0.0370 (25)	0.2727 (24)	0.0908
C2	−0.3808 (19)	0.1116 (14)	0.2566 (13)	0.1531
C3	−0.4429 (22)	−0.0682 (24)	0.1363 (23)	0.0801
C4	−0.4274 (14)	−0.1674 (14)	0.0986 (13)	0.1134
C1′	−0.3607 (22)	0.0161 (23)	0.2214 (22)	0.0753
C3′	−0.3483 (23)	−0.0951 (21)	0.2785 (22)	0.0784

[a] Calculated standard deviations are indicated in parentheses. [b] The equivalent isotropic thermal parameters are in units of square angstroms.

carbon atoms but were not refined. The final R value was 0.044, and R_w was 0.044. In the last cycle of refinement, all parameter shifts were less than 10% of their esd.

$[(C_6H_5)_4P]_4Fe_6S_6Cl_6[Mo(CO)_3]_2·2CH_3CN$ (II). This structure was also solved by direct methods using the SOLV routine of SHELXTL84. As in the structure of I, the anion in II is located on a crystallographic center of inversion at 0, 0, 0 in space group $P2_1/n$. The positions of the molybdenum and the three iron atoms were initially located. Phasing on these atoms revealed the positions of the remaining atoms in the anion and of the non-hydrogen atoms in the cations. There are two tetraphenylphosphonium cations in the asymmetric unit, and both are located in general positions. The CH_3CN molecule of solvation was also found, and all non-hydrogen atoms in the asymmetric unit were refined with isotropic temperature factors to a conventional R value of 0.10. The refinement process then continued with full-matrix least-squares techniques after the assignment of anisotropic temperature factors to all atoms in the anion. The positions of the hydrogen atoms in the cation were calculated at 0.95 Å from the carbon atoms, and the hydrogen atoms were included in the structure factor calculations but were not refined. The final R value, after the refinement calculations had converged, was 0.062, and R_w was 0.061. During the last cycle of refinement, all parameter shifts were less than 10% of their esd.

$[(C_2H_5)_4N]_3Fe_6S_6Cl_6[Mo(CO)_3]_2$ (III). The solution of the structure was accomplished with the use of the direct-methods routine SOLV of the SHELXTL84 package of crystallographic programs.

There is one crystallographically independent anion in III, which in space group $R\bar{3}c$ (No. 167) is situated on a special position (0, 0, 0;

Table V. Fractional Atomic Coordinates[a,b] and Equivalent Isotropic Thermal Parameters for the Non-Hydrogen Atoms in $[(C_2H_5)_4N]_3Fe_6S_6Br_6[Mo(CO)_3]_2$ (IV)

atom	x	y	z	U
Mo1	0.4449 (01)	0.6650 (01)	−0.0917 (01)	0.0397
Fe1	0.4219 (01)	0.4629 (01)	−0.1317 (01)	0.0405
Fe2	0.6428 (01)	0.5929 (01)	−0.0274 (01)	0.0391
Fe3	0.3817 (01)	0.5896 (01)	0.0797 (01)	0.0392
S1	0.5298 (03)	0.6728 (02)	0.0589 (02)	0.0410
S2	0.3084 (03)	0.5417 (02)	−0.0473 (02)	0.0396
S3	0.5718 (03)	0.5444 (03)	−0.1565 (02)	0.0406
Br1	0.3322 (01)	0.4074 (01)	−0.2560 (01)	0.0665
Br2	0.7957 (01)	0.6809 (01)	−0.0449 (01)	0.0701
Br3	0.2581 (01)	0.6671 (01)	0.1652 (01)	0.0604
CX1	0.3812 (12)	0.6751 (11)	−0.2078 (11)	0.0577
O1	0.3465 (09)	0.6839 (09)	−0.2766 (08)	0.0802
CX2	0.5408 (11)	0.7643 (11)	−0.1275 (10)	0.0540
O2	0.5951 (09)	0.8255 (08)	−0.1476 (09)	0.0945
CX3	0.3492 (11)	0.7686 (11)	−0.0565 (10)	0.0481
O3	0.2998 (08)	0.8313 (08)	−0.0381 (07)	0.0693
N1	0.5173 (09)	0.9355 (08)	0.2513 (08)	0.0482
C1	0.4751 (11)	1.0023 (10)	0.3164 (10)	0.0547
C2	0.5520 (13)	1.0650 (12)	0.3606 (12)	0.0854
C3	0.6051 (10)	0.8760 (10)	0.2923 (11)	0.0543
C4	0.5750 (12)	0.8244 (12)	0.3739 (12)	0.0800
C5	0.5618 (13)	0.9877 (11)	0.1762 (12)	0.0726
C6	0.6072 (15)	0.9288 (13)	0.1037 (12)	0.0954
C7	0.4297 (11)	0.8700 (10)	0.2194 (11)	0.0574
C8	0.3412 (13)	0.9195 (13)	0.1750 (12)	0.0874
N2	0.0 (-)	0.0 (-)	0.0 (-)	0.0374
C9	−0.0711 (21)	0.0838 (21)	0.0065 (19)	0.0515
C10	−0.0470 (43)	0.1584 (42)	−0.0599 (36)	0.0587
C11	−0.0004 (26)	0.0442 (24)	0.0851 (22)	0.0759
C12	0.1011 (29)	0.0790 (27)	0.1273 (25)	0.0604
C13	−0.0340 (22)	−0.0694 (22)	0.0709 (20)	0.0595
C14	0.0436 (46)	−0.1549 (46)	0.0813 (38)	0.0820
C15	0.1150 (26)	0.0308 (26)	0.0197 (24)	0.0791
C16	0.1372 (33)	0.0754 (33)	0.0990 (31)	0.0909

[a] Calculated standard deviations are indicated in parentheses. [b] The equivalent isotropic thermal parameters are in units of square angstroms.

Wyckoff notation b, point symmetry $\bar{3}$). The molybdenum atom of the unique fragment was initially located from direct methods followed by the appearance of the sulfur atom. Subsequent location of the iron atom as well as the terminal chlorine atom completed the [Mo–Fe–S–Cl] fragment of the $[Mo_2Fe_6S_6]^{3+}$ core. The nitrogen atom of the tetraethylammonium cation is located on the 2-fold axis at $(x, \frac{1}{2} - x, \frac{1}{4})$ with $x = -0.439\,12$ (Wyckoff notation e).

The rest of the non-hydrogen atoms were found with successive electron density difference Fourier maps following least squares of the input atomic coordinates. The refinement of all atoms in the asymmetric unit using isotropic temperature factors gave a conventional R value of 0.079.

The cation in the asymmetric unit was found to be positionally disordered with approximate 50% occupancy. The refinement process then continued (full matrix least squares), assigning anisotropic temperature factors to all non-hydrogen, nondisordered atoms in the asymmetric unit. At this stage, the hydrogen atom positions in the asymmetric unit were calculated. In the final cycle of refinement, they were included in the structure factor calculation but were not refined. The final R value was 0.049, and the weight R value was 0.05. During the last cycle of refinement, all parameter shifts were less than 10% of their estimated standard deviation.

$[(C_2H_5)_4N]_3Fe_6S_6Br_6[Mo(CO)_3]_2$ (IV). The structure was solved by the direct-methods routine SOLV of the SHELXTL84 crystallographic program package.

The $[Fe_6S_6Br_6(Mo(CO)_3)_2]^{3-}$ anion is required by symmetry to reside on a crystallographic inversion center. The molybdenum and the three unique iron atoms were initially located. A subsequent Fourier map calculation revealed the three crystallographically unique sulfur atoms, thus completing the [MoFe$_3$S$_3$] unique fragment of the $[Mo_2Fe_6S_6]^{3+}$ core. The rest of the non-hydrogen atoms were found with successive electron density difference Fourier maps following least squares of the input atomic coordinates.

The refinement of all the atoms in the asymmetric unit using isotropic temperature factors gave a conventional R value of 0.09.

One of the tetraethylammonium cations resides on a general position, and the other resides on a center of symmetry. As a result, the latter is subject to a 2-fold disorder. The type of disorder is identical with the

one encountered in $[(C_2H_5)_4N]_3[Fe_6S_6(OC_6H_4-p-CH_3)_6]^{17e}$ and $[(C_2H_5)_4N]_3[Fe_6S_6Br_6]\cdot CH_3CN^{17e}$ and was treated similarly.

The refinement process then continued (full-matrix least-squares techniques) assigning anisotropic temperature factors to all non-hydrogen, nondisordered atoms in the asymmetric unit. At this stage, the hydrogen atom positions in the asymmetric unit were calculated. In the final refinement, they were included in the structure factor calculation but were not refined. The final R value was 0.04, and the weighted R was 0.04. During the last cycle of refinement, all parameter shifts were 10% of their estimated standard deviation.

d. Crystallographic Results. The final atomic positional and thermal parameters for the anions in I–IV with standard deviations derived from the inverse matrices of the least-squares refinements are compiled in Tables II–V. Similar parameters for the cations and the hydrogen atoms have been deposited as supplementary material. Intramolecular distances and angles for all the anions are included in Table IX with the common labeling scheme shown in Figure 2.

Results and Discussion

Synthesis. The syntheses of all complexes were carried out under strictly anaerobic and moisture-free conditions. The synthesis of the $[Fe_4S_4X_4]^{2-}$ clusters (X = Cl⁻, Br⁻) has been reported previously[20] by the reaction of the $[Fe_4S_4(SR)_4]^{2-}$ clusters (R = t-Bu, Ph) with PhCOX in CH₃CN solution. The iodo analogue was obtained[20] by substitution of Cl⁻ in the $[Fe_4S_4Cl_4]^{2-}$ cluster using NaI. Herein we report a new synthetic procedure for obtaining the X = Br⁻, I⁻ clusters, in very good yields, by a simpler spontaneous self-assembly process.

The $[Fe_6S_6Cl_6(Mo(CO)_3)_2]^{4-}$ tetraanion can be obtained in good yields by two general synthetic procedures. These are (a) direct synthesis from the reaction of the $[Fe_6S_6Cl_6]^{3-}$ prismane with $Mo(CO)_3(CH_3CN)_3$ in a 1:4 molar ratio and (b) reorganization of either $[Fe_2S_2Cl_4]^{2-}$ [20] or $[Fe_4S_4Cl_4]^{2-}$ [20] in the presence of $Mo(CO)_3(CH_3CN)_3$ in CH₃CN or CH₃CH₂CN solutions. In the first of these procedures, the excess $Mo(CO)_3(CH_3CN)_3$ is needed for the complete reduction of the trianionic adduct that forms initially. The $Mo(CO)_3(CH_3CN)_3$ reagent undergoes reversible oxidation at +0.30 V in CH₃CN solution and is an effective reducing agent for the $[Fe_6S_6Cl_6(Mo(CO)_3)_2]^{3-}$ trianion, which shows a reversible 3–/4– couple at +0.05 V (vide infra). The reorganization reactions of the $[Fe_2S_2Cl_4]^{2-}$ or $[Fe_4S_4Cl_4]^{2-}$ clusters that eventually lead to the formation of the $[Fe_6S_6Cl_6(Mo(CO)_3)_2]^{4-}$ cluster demonstrate the remarkable relative thermodynamic stability of the latter. These reactions could be visualized as the direct fusion of three solvated $[Fe_2S_2Cl_2]^-$ units on a $Mo(CO)_3$ template. The $[Fe_2S_2Cl_4]^{3-}$ units, or $[Fe_2S_2Cl_2]^-$ units in a solvated form, couple to form the $[Fe_4S_4Cl_4]^{2-}$ cubane in the known[20] irreversible reduction of the $[Fe_2S_2Cl_4]^{2-}$ dimer. The $[Fe_6S_6X_6(Mo(CO)_3)_2]^{4-}$ clusters (X = Br⁻, I⁻) can be obtained either from the $[Fe_4S_4X_4]^{2-}$ cubanes as previously described or, in the case of X = I⁻, by substitution of the Cl⁻ ligands in the $[Fe_6S_6Cl_6(Mo(CO)_3)_2]^{4-}$ cluster using NaI.

The trianionic $[Fe_6S_6X_6(Mo(CO)_3)_2]^{3-}$ adducts (X = Cl⁻, Br⁻) can be obtained by any of the following procedures: (a) direct reaction of the appropriate prismanes with $Mo(CO)_3(CH_3CN)_3$ in CH₃CN or $C_2H_4Cl_2$ in a 1:2 molar ratio; (b) reaction of the $[Fe_6S_6(OAr)_6(Mo(CO)_3)_2]^{3-}$ analogues[18a] with either C_6H_5COCl or C_6H_5COBr in CH₃CN solution in 1:6 molar ratios; (c) oxidation of the corresponding tetraanions with $(C_5H_5)_2FePF_6$ in CH₃CN or CH₂Cl₂ solution. Two different crystalline modifications were isolated for the $(Et_4N)_3[Fe_6S_6Br_6(Mo(CO)_3)_2]$ salt. The rhombohedral modification is X-ray isomorphous to the Cl analogue and is obtained when 1.1 equiv of $(C_5H_5)_2FePF_6$/equiv of the tetraanion percursor is used. A monoclinic modification is obtained when the small excess of oxidizing agent (1.5 equiv) is used in the synthesis in an otherwise similar procedure. The structure of the monoclinic modification was determined and is reported herein (vide infra). The iodo derivatives of the trianionic adducts are conveniently obtained by the substitution of the Cl⁻ ligands in the chloro analogue using NaI. The $[Fe_6S_6X_6(W(CO)_3)_2]^{3-}$ clusters (X = Cl⁻, Br⁻) are obtained readily by procedure b above and the corresponding tetraanions with $R_4N^+BH_4^-$ reduction in CH₃CN solution.

Electronic and Infrared Spectra. The electronic spectra of the

Table VI. Electronic Spectra[a] of the $[Fe_6S_6X_6(M(CO)_3)_2]^{n-}$ (n = 3, 4; X = Cl⁻, Br⁻, I⁻; M = Mo, W) Series

compd	λ_{max}, nm	ϵ, M⁻¹ cm⁻¹
$[(C_2H_5)_4N]_3Fe_6S_6Cl_6[Mo(CO)_3]_2$	460	11 455
$[(C_2H_5)_4N]_3Fe_6S_6Br_6[Mo(CO)_3]_2$	314	22 136
	470 (sh)	~9938
$[(C_6H_5)_4P]_3Fe_6S_6I_6[Mo(CO)_3]_2$	380	~22 000
	420 (sh)	~21 612
$[(C_2H_5)_4N]_4Fe_6S_6Cl_6[Mo(CO)_3]_2$	370 (sh)	~8929
	470 (sh)	~12 106
$[(C_2H_5)_4N]_4Fe_6S_6Br_6[Mo(CO)_3]_2$	296 (sh)	~34 772
	470 (sh)	~13 030
$[(C_6H_5)_4P]_4Fe_6S_6I_6[Mo(CO)_3]_2$	364	17 770
$[(C_2H_5)_4N]_3Fe_6S_6Cl_6[W(CO)_3]_2$	380 (sh)	...
	490 (sh)	...
$[(C_2H_5)_4N]_3Fe_6S_6Br_6[W(CO)_3]_2$	306	...
	470 (sh)	
$[(C_2H_5)_4N]_4Fe_6S_6Cl_6[W(CO)_3]_2$	370 (sh)	...
	480 (sh)	
$[(C_2H_5)_4N]_4Fe_6S_6Br_6[W(CO)_3]_2$	480 (sh)	...

[a] Obtained in CH₃CN solutions.

Table VII. Infrared Absorptions of $[Fe_6S_6X_6(M(CO)_3)_2]^{3-,4-}$ (M = Mo, W; X = Cl⁻, Br⁻, I⁻) Clusters

	ν(C–O), cm⁻¹	
compd	solid state[a]	soln[b]
$[(C_2H_5)_4N]_3Fe_6S_6Cl_6[Mo(CO)_3]_2$	1925	1945
		1918
$[(C_6H_5)_4P]_3Fe_6S_6Cl_6[Mo(CO)_3]_2$	1932	1945
	1892	1918
$[(C_2H_5)_4N]_3Fe_6S_6Br_6[Mo(CO)_3]_2$ (R)	1925	1948
		1912
$[(C_2H_5)_4N]_3Fe_6S_6Br_6[Mo(CO)_3]_2$ (M)	1937	1948
	1902	1912
	1887	
$[(C_2H_5)_4N]_3Fe_6S_6I_6[Mo(CO)_3]_2$	1938	1949
	1916	1905
$[(C_6H_5)_4P]_3Fe_6S_6I_6[Mo(CO)_3]_2$	1936	1948
	1904	1905
$[(C_2H_5)_4N]_3Fe_6S_6Cl_6[W(CO)_3]_2$	1919	1944
		1899
$[(C_2H_5)_4N]_3Fe_6S_6Br_6[W(CO)_3]_2$	1919	1947
		1907
$[(C_2H_5)_4N]_4Fe_6S_6Cl_6[Mo(CO)_3]_2$	1897	1908
	1834	1847
$[(C_2H_5)_4N]_4Fe_6S_6Br_6[Mo(CO)_3]_2$	1906	1912
	1852	1852
$[(C_2H_5)_4N]_4Fe_6S_6I_6[Mo(CO)_3]_2$	1912	1917
	1857	1857
$[(C_6H_5)_4P]_4Fe_6S_6I_6[Mo(CO)_3]_2$	1903	1920
	1846	1857
$[(C_2H_5)_4N]_4Fe_6S_6Cl_6[W(CO)_3]_2$	1891	
	1833	
$[(C_2H_5)_4N]_4Fe_6S_6Br_6[W(CO)_3]_2$	1895	
	1845	

[a] CsI pellet. [b] In CH₃CN solution.

adducts (Table VI) generally show broad absorptions in the UV and visible regions. Within this envelope of absorptions, shoulders, and occasionally distinct maxima, can be identified. These spectral features are presented in Table VI as characterization data. The electronic spectra of the $[Fe_6S_6X_6]^{3-}$ parent prismanes show absorption maxima at 270, 306, and 350 nm, respectively, for X = Cl⁻, Br⁻, and I⁻. These absorptions that have been tentatively assigned previously[17c] to X → core charge-transfer excitations are also apparent in the spectra of the prismane adducts. In the latter, these absorptions appear to be bathochromically shifted. Such a low-energy shift would be expected if S → Mo charge transfer indirectly depletes electron density from the iron atoms. A feature in the spectra of the adducts that is not observed in the spectra of the parent prismanes is a broad absorption between 400 and 500 nm. This feature may be attributable, at least in part, to S → Mo charge-transfer excitations.

Other than this phenomenological account of the electronic spectra, any further discussion or reliable assignments are pre-

Table VIII. Cyclic Voltammetric Data for the $[Fe_6S_6X_6(M(CO)_3)_2]^{3-/4-\,a}$ (X = Cl⁻, Br⁻, I⁻; M = Mo, W) Cluster Series in $CH_2Cl_2{}^b$

	3−/4− couple			4−/5− couple		
cluster	$E_{1/2}$, V	ΔE, mV	i_{p_c}/i_{p_a}	$E_{1/2}$, V	ΔE, mV	i_{p_a}/i_{p_c}
$[(C_2H_5)_4N]_3Fe_6S_6Cl_6[Mo(CO)_3]_2$	+0.05	92	1.00	−0.54	86	1.00
$[(C_2H_5)_4N]_3Fe_6S_6Br_6[Mo(CO)_3]_2$	+0.08	90	0.99	−0.50	90	1.00
$[(C_6H_5)_4P]_3Fe_6S_6I_6[Mo(CO)_3]_2$	+0.08	121	1.00	−0.49	120	0.94
$[(C_2H_5)_4N]_3Fe_6S_6(OC_6H_4\text{-}p\text{-}CH_3)_6[Mo(CO)_3]_2{}^{17g}$	−0.35	152	1.00	−0.89	193	1.00
$[(C_2H_5)_4N]_3Fe_6S_6(SC_6H_5)_6[Mo(CO)_3]_2{}^{17g}$	−0.30	110	1.00	−0.75	108	1.00
$[(C_2H_5)_4N]_3Fe_6S_6Cl_6[W(CO)_3]_2$	+0.04	84	1.00	−0.55	103	1.00
$[(C_2H_5)_4N]_3Fe_6S_6Br_6[W(CO)_3]_2$	+0.06	96	1.00	−0.51	103	1.00
$[(C_2H_5)_4N]_3Fe_6S_6(OC_6H_4\text{-}p\text{-}CH_3)_6[W(CO)_3]_2{}^{17g}$	−0.38	141	0.96	−0.87	130	0.96
$[(C_2H_5)_4N]_3Fe_6S_6(SC_6H_5)_6[W(CO)_3]_2{}^{17g}$	−0.31	114	0.95	−0.73	114	1.00

a For all measurements the scan rate was 200 mV/s. *b* Normally the $[(C_2H_5)_4N]^+$ salts of the above clusters are not soluble in this solvent. In the presence of excess $(n\text{-}Bu_4N)ClO_4$ as supporting electrolyte, however, they readily go into solution.

cluded by the complexity of the chromophores and the apparent convolution of the electronic absorptions.

The infrared spectra of the $[Fe_6S_6X_6(M(CO)_3)_2]^{n-}$ clusters have been obtained in the solid state and in CH_3CN solution. In the region between 1800 and 1950 cm⁻¹, all of these complexes exhibit two strong C−O absorptions (Table VII). These absorption bands can be assigned to the asymmetric E and the symmetric A vibrational modes of the $M(CO)_3$ units with C_{3v} local symmetry. A comparison of the C−O vibrational frequencies between the tetraanionic and the trianionic clusters shows that, in the latter, these frequencies are shifted to higher energies. Specifically, these differences for the A mode are 37, 36, and 32 cm⁻¹ for X = Cl⁻, Br⁻, and I⁻, respectively. The corresponding differences for the E mode are 71, 60, and 48 cm⁻¹. These data are consistent with both structural and ⁵⁷Fe Mössbauer data that suggest partial oxidation of the Mo atoms in the trianionic adducts (vide infra). The C−O frequencies of the $[Fe_6S_6X_6(M(CO)_3)_2]^{n-}$ adducts in solution resemble those in the tricarbonyl(1,4,7-trithiacyclononane)molybdenum(0) complex[23,24] (1935, 1825 cm⁻¹), the $[(C_2H_5)_2S]_3Mo(CO)_3$ complex[25] (1930, 1826 cm⁻¹), and the $(C_4H_8\text{-}S)_3Mo(CO)_3$ complex[25] (1925, 1821 cm⁻¹). It should be noted that, in the $[Fe_6S_6(OAr)_6(Mo(CO)_3)_2]^{3-}$ adduct,[18a] the C−O frequencies are found at 1915 and 1860 cm⁻¹, considerably lower than those in the corresponding halo trianions (Table VII).

Electrochemical Measurements. The results of cyclic voltammetric studies (on a Pt electrode in CH_2Cl_2 solution) on the $[Fe_6S_6X_6(M(CO)_3)_2]^{n-}$ clusters are summarized in Table VIII. All complexes show two reversible waves round +0.05 and −0.50 V that correspond to the 3−/4− and 4−/5− couples. The half-wave potentials for the 3−/4− and 4−/5− couples are between 300 and 400 mV more positive than the corresponding potentials for the thioaryl or aryloxy analogue prismane adducts. These differences account for the ready reduction of the 3− halo clusters, in the presence of the mildly reducing $(CH_3CN)_3M(CO)_3$ agents, during the synthesis of the clusters. Positive shifts in redox potentials, following the substitution of terminal thioaryl or aryloxy ligands by halides, have also been found with the parent $[Fe_6S_6(L)_6]^{n-}$ prismanes[17] and the $[Fe_4S_4(L)_4]^{n-}$[20] cubane clusters.

A slight but systematic shift of the redox potentials to more positive values is detected in the order $E_{1/2}(Cl) > E_{1/2}(Br) > E_{1/2}(I)$ for both the 3−/4− and 4−/5− couples. Such a trend has been identified previously for the 2−/3− couples in the $[Fe_4S_4X_4]^{2-}$[20] and the $[Fe_6S_6X_6]^{3-}$ clusters[17d] (X = Cl⁻, Br⁻, I⁻). Substitution of Mo by W in the $[Fe_6S_6X_6(M(CO)_3)_2]^{n-}$ clusters results in a slight shift of the redox potentials to more negative values. This behavior has a precedent in the electrochemistry of the $[M_2Fe_6S_9(SEt)_8]^{3-}$ double-cubane clusters[26] (M = Mo, W) and the $[(PhS)_2FeS_2MS_2]^{2-}$ and $[(S_5)_2FeS_2MS_2]^{2-}$ dimers.[27] A

multielectron irreversible oxidation is observed for the $[Fe_6S_6X_6(M(CO)_3)_2]^{n-}$ clusters at potentials more positive than +0.55 V. The products of this oxidative degradation have not been identified to date. At present, we are attempting to characterize these oxidation products, cognizant of the fact that the oxidative degradation of the $[Fe_4S_4X_4]^{2-}$ clusters[17b] leads to the nearly quantitative formation of the $[Fe_6S_6X_6]^{2-}$ clusters. The reversibility and low negative values for the 4−/5− reduction of the adducts suggest that the corresponding pentaanions should be chemically accessible. To date, we have been unable to isolate the chemical reduction products in any tractable form.

Description of the Structures. In all structures, the Et_4N^+ and Ph_4P^+ cations are well separated from the anions and are unexceptional. As such, they will not be considered further.

The $Mo_2Fe_6S_6$ cages in I, II, and IV possess idealized D_{3d} symmetry. In the structure of III, the anion has crystallographically required $\bar{3}$ symmetry. The topological relationship of the Fe_6S_6 prismane cores to the M_8S_6 cubic units in the naturally occurring pentlandite minerals (Figure 1) has been described previously in detail.[17] In this context, the $[Fe_6S_6X_6(Mo(CO)_3)_2]^{n-}$ anions in I–IV (Figure 2) are best described in terms of $[Fe_6S_6X_6]^{n-}$ prismane-type units capped at each of the two Fe_3S_3 hexagonal "chairs" by $Mo(CO)_3$ moieties. The resulting $Mo_2Fe_6S_6$ rhombohedra (Figure 2) to a first approximation are structurally analogous to the M_8S_6 rhombic dodecahedral cores found in the pentlandite-type solids such as Co_9S_8,[28] $(Ni,Fe)_9S_8$,[29a] and $(Ni,Fe)_8AgS_8$,[29b] in the djerfisherite-like $(K_6Cl)[Li\text{-}((Fe_8S_6)S_{8/3})_3]$,[30,32] in bartonite, $(K_6Cl)_2[(Fe_8S_6)S_{8/3}]_6$,[31,32] in the Co_8S_6 core in the $[Co_8S_6(SPh)_8]^{4-}$ cluster,[15] and in the Fe_8S_6 core in the $[Fe_8S_6I_8]^{3-}$ cluster.[16]

In each of the four anions in I–IV the Mo_2Fe_6 rhombohedra are elongated along the body diagonal that contains the two molybdenum atoms. This elongation is a direct consequence of both metrical differences between the Mo−S and Fe−S bond lengths and distinct structural changes within the Fe_6S_6 subunits.

A comparison of the Fe_6S_6 cores in the $[Fe_6S_6X_6]^{n-}$ prismanes[17] to those in the $[Fe_6S_6X_6(Mo(CO)_3)_2]^{n-}$ adducts (Table IX) shows the latter elongated along the idealized $\bar{3}$ axes. Specifically, the Fe−S bonds parallel to the $\bar{3}$ axes in I–IV in the range from 2.311 (4) to 2.333 (3) Å are significantly longer than the corresponding bonds in the $[Fe_6S_6X_6]^{n-}$ prismanes (X = Cl⁻, Br⁻, n = 3; X = Cl⁻, n = 2; range 2.269 (2)–2.284 (3) Å). This "stretching" of the Fe_6S_6 cores that apparently follows the addition of the $Mo(CO)_3$ units is also apparent in the Fe−S−Fe angles within the Fe_3S_3 hexagons. In the adducts, these angles range from 110.9 (3) to 111.7 (7)° and are slightly smaller than the corresponding angles in the prismanes (range 113.2 (3)–114.9 (5)°). The mean values of the Fe−S bond lengths in I–IV at 2.302 (8), 2.300 (8), 2.292 (10), and 2.290 (7) Å are indistinguishable within 1 σ and are similar to the Fe−S bonds in bartonite (2.294 Å), $K_6Li\text{-}$

(23) Ashby, M. T.; Lichtenberger, D. L. *Inorg. Chem.* **1985**, *24*, 636–638.
(24) Backes-Dahmann, G.; Wieghardt, K. *Inorg. Chem.* **1985**, *24*, 4049–4054.
(25) Cotton, F. A.; Zingales, F. *Inorg. Chem.* **1962**, *1*, 145.
(26) Wolff, T. E.; Power, P. P.; Frankel, R. B.; Holm, R. H. *J. Am. Chem. Soc.* **1980**, *102*, 4694.
(27) Coucouvanis, D.; Stremple, P.; Simhon, E. D.; Swenson, D.; Baenziger, N. C.; Draganjac, M.; Chan, L. T.; Simopoulos, A.; Papaefthymiou, V.; Kostikas, A.; Petrouleas, V. *Inorg. Chem.* **1983**, *22*, 293.

(28) Rajamani, V.; Prewitt, C. T. *Can. Mineral.* **1975**, *13*, 75.
(29) (a) Rajamani, V.; Prewitt, C. T. *Can. Mineral.* **1973**, *12*, 178. (b) Hall, S. R.; Stewart, J. M. *Can. Mineral.* **1973**, *12*, 169.
(30) Tani, B. *Am. Mineral.* **1977**, *62*, 819.
(31) Evans, H. T.; Clark, J. R. *Am. Mineral.* **1981**, *66*, 376.
(32) Burdett, J. K.; Miller, G. J. *J. Am. Chem. Soc.* **1987**, *109*, 4081–4091.

Table IX. Selected Distances (Å) and Angles (deg) in the Anions of $(Et_4N)_4Fe_6S_6Cl_6[Mo(CO)_3]_2\cdot2CH_3CN$ (I), $(Ph_4P)_4Fe_6S_6Cl_6[Mo(CO)_3]_2\cdot2CH_3CN$ (II), $(Et_4N)_3Fe_6S_6Cl_6[Mo(CO)_3]_2$ (III), and $(Et_4N)_3Fe_6S_6Br_6[Mo(CO)_3]_2$ (IV)

	I[a]	II[b]	III[c]	IV[d]		I[a]	II[b]	III[c]	IV[d]
					Distances[e,f]				
Mo1–Fe1	2.980 (1)	2.942 (1)	2.930 (2)	2.954 (2)	Fe1–S2	2.288 (2)	2.292 (3)		2.262 (4)
Mo1–Fe2	3.031 (2)	3.016 (2)		2.913 (2)	Fe1–S3	2.292 (2)	2.286 (3)		2.286 (4)
Mo1–Fe3	3.004 (1)	3.012 (2)		2.971 (2)	Fe2–S1	2.281 (2)	2.274 (3)		2.283 (4)
mean	3.005 (15)	2.99 (2)		2.95 (2)	Fe2–S3	2.287 (2)	2.286 (3)		2.288 (4)
					Fe3–S1	2.279 (2)	2.280 (3)		2.269 (4)
Mo1–S1	2.611 (2)	2.620 (2)	2.581 (3)	2.557 (4)	Fe3–S2	2.292 (2)	2.283 (3)		2.270 (4)
Mo1–S2	2.620 (2)	2.610 (3)		2.579 (4)	Fe1–S1			2.280 (4)	
Mo1–S3	2.625 (2)	2.594 (3)		2.577 (4)	Fe1–S1′			2.284 (4)	
mean	2.619 (4)	2.608 (8)		2.571 (7)	mean	2.287 (2)	2.284 (3)		2.276 (4)
Mo1–CX1	1.954 (10)	1.960 (11)	2.02 (2)	1.97 (2)	S1–S2	3.808 (3)	3.804 (3)		3.767 (5)
Mo1–CX2	1.969 (9)	1.942 (13)		1.96 (2)	S2–S3	3.844 (3)	3.848 (3)		3.799 (5)
Mo1–CX3	1.950 (10)	1.926 (13)		2.00 (2)	S3–S1	3.789 (3)	3.785 (3)		3.830 (5)
mean	1.958 (10)	1.943 (13)		1.98 (2)	S1–S1″			3.830 (5)	
					mean	3.81 (2)	3.81 (2)		3.80 (2)
Fe1–Fe2	3.783 (2)	3.767 (2)		3.743 (3)					
Fe2–Fe3	3.805 (2)	3.788 (2)		3.759 (3)	S1–S2′	3.683 (3)	3.734 (3)		3.700 (5)
Fe1–Fe3	3.766 (2)	3.742 (2)		3.763 (3)	S2–S3′	3.708 (3)	3.686 (3)		3.695 (5)
Fe1–Fe1′			3.760 (3)		S3–S1′	3.718 (3)	3.710 (3)		3.682 (5)
mean	3.785 (11)	3.766 (13)		3.755 (6)	S1–S1′			3.686 (6)	
					mean	3.703 (10)	3.71 (2)		3.693 (6)
Fe1–Fe2′	2.781 (2)	2.722 (2)		2.714 (3)	CX1–O1	1.151 (10)	1.170 (11)		1.153 (17)
Fe2–Fe3′	2.763 (2)	2.780 (2)		2.736 (3)	CX2–O2	1.153 (10)	1.166 (14)		1.161 (15)
Fe3–Fe1′	2.740 (2)	2.739 (2)		2.749 (3)	CX3–O3	1.168 (10)	1.175 (13)		1.133 (15)
Fe1–Fe1″			2.742 (3)		CX1–O1			1.14 (2)	
mean	2.761 (12)	2.75 (2)		2.733 (10)	mean	1.157 (10)	1.170 (14)		1.149 (17)
Fe1–S1′	2.329 (3)	2.333 (3)		2.316 (4)	Fe1–(Cl,Br)1	2.244 (2)	2.265 (3)		2.362 (3)
Fe2–S2′	2.333 (3)	2.341 (3)		2.317 (4)	Fe2–(Cl,Br)2	2.248 (2)	2.263 (3)		2.351 (2)
Fe3–S3′	2.336 (3)	2.324 (3)		2.320 (4)	Fe3–(Cl,Br)3	2.244 (2)	2.237 (3)		2.350 (2)
Fe1–S1″			2.311 (4)		Fe1–Cl1			2.225 (4)	
mean	2.333 (3)	2.333 (5)		2.318 (4)	mean	2.245 (2)	2.255 (9)		2.354 (4)
					Angles[e,f]				
S1–Mo1–S2	93.4 (1)	93.3 (1)		94.3 (1)	S1–Fe1′–S2′	105.8 (1)	107.7 (1)		107.8 (1)
S1–Mo1–S3	92.7 (1)	93.1 (1)		96.5 (1)	S1–Fe1′–S3′	107.1 (1)	106.9 (1)		106.3 (1)
S2–Mo1–S3	94.2 (1)	95.4 (1)		94.9 (1)	S2–Fe2′–S1′	105.9 (1)	108.0 (1)		107.1 (1)
S1–Mo1–S1′			95.8 (1)		S2–Fe2′–S3′	106.7 (1)	105.6 (1)		106.7 (1)
mean	93.4 (4)	93.9 (7)		95.2 (7)	S3–Fe3′–S1′	107.3 (1)	107.4 (1)		106.7 (1)
					S3–Fe3′–S2′	106.5 (1)	106.3 (1)		107.2 (1)
Fe2–S1–Fe3	113.1 (1)	112.5 (1)		111.3 (2)	S1–Fe1–S1′			106.8 (3)	
Fe3–S2–Fe1	110.7 (1)	109.8 (1)		112.3 (2)	S1–Fe1–S1″			106.6 (3)	
Fe1–S3–Fe2	111.4 (1)	111.0 (1)		109.8 (2)	mean	106.6 (2)	107.0 (4)		107.0 (2)
Fe1–S1–Fe1′			110.9 (3)						
mean	111.7 (7)	111.1 (8)		111.1 (7)	(Cl,Br)1–Fe1–S2	112.2 (1)	110.1 (1)		108.5 (1)
					(Cl,Br)1–Fe1–S3	110.9 (1)	110.7 (1)		116.2 (1)
Fe1–S1′–Fe2′	74.2 (1)	72.4 (1)		72.3 (1)	(Cl,Br)2–Fe2–S1	110.9 (1)	108.0 (1)		109.9 (1)
Fe1–S1′–Fe3′	73.0 (1)	72.8 (1)		73.7 (1)	(Cl,Br)2–Fe2–S3	112.8 (1)	117.0 (1)		112.9 (1)
Fe2–S2′–Fe1′	74.0 (1)	71.9 (1)		72.7 (1)	(Cl,Br)3–Fe3–S1	107.7 (1)	110.1 (1)		114.2 (1)
Fe2–S2′–Fe3′	73.4 (1)	73.9 (1)		73.2 (1)	(Cl,Br)3–Fe3–S2	114.3 (1)	115.0 (1)		110.2 (1)
Fe3–S3′–Fe1′	72.6 (1)	72.9 (1)		73.3 (1)	Cl1–Fe1–S1′			109.3 (1)	
Fe3–S3′–Fe2′	73.4 (1)	74.2 (1)		72.8 (1)	Cl1–Fe1–S1″			112.1 (1)	
Fe1–S1–Fe1′			73.3 (3)		mean	111.5 (9)	111.8 (14)		112.0 (12)
Fe1–S1–Fe1′			73.3 (3)						
mean	73.4 (2)	73.0 (4)		73.0 (2)	S1′–Fe1–(Cl,Br)1	106.0 (1)	106.7 (1)	107.7 (1)	103.9 (1)
					S2′–Fe2–(Cl,Br)2	108.0 (1)	105.5 (1)		105.9 (1)
S2–Fe1–S3	114.1 (1)	114.4 (1)		113.3 (1)	S3′–Fe3–(Cl,Br)3	107.8 (1)	104.4 (1)		105.8 (1)
S3–Fe2–S1	112.1 (1)	112.2 (1)		113.8 (1)	mean	107.3 (6)	105.5 (7)		105.2 (7)
S1–Fe3–S2	112.9 (1)	112.9 (1)		112.2 (1)					
S1–Fe1–S1′			114.1 (3)		Fe1–Mo1–Fe2	78.00 (1)	78.40 (1)		79.30 (2)
mean	113.0 (6)	113.2 (6)		113.1 (5)	Fe2–Mo1–Fe3	78.20 (1)	77.90 (1)		79.40 (2)
					Fe3–Mo1–Fe1	78.00 (1)	77.90 (1)		78.80 (2)
					Fe1–Mo1–Fe1′			79.80 (1)	
					mean	78.07 (7)	78.1 (2)		79.2 (2)
					Fe2–Fe1–Fe3	60.50 (1)	60.60 (1)		60.10 (3)
					Fe1–Fe2–Fe3	59.50 (1)	59.40 (1)		60.21 (3)
					Fe2–Fe3–Fe1	60.00 (1)	60.00 (1)		59.68 (3)
					Fe1′–Fe1–Fe1″			60.00 (1)	
					mean	60.0 (3)	60.0 (4)		60.0 (2)

[a] For the nondisordered cation (N1) in I, the N–C bonds are within the range 1.50 (1)–1.52 (1) Å with a mean value of 1.51 (1) Å. The C–C bonds are within the range 1.49 (1)–1.51 (1) Å with a mean value of 1.50 (1) Å. The C_i–N1–C_j angles are found between 102.6 (7) and 113.7 (7)° with a mean value of 110 (2)°. For the disordered cation (N2) in I, the N–C bonds are within the range 1.40 (2)–1.74 (3) Å with a mean value of 1.54 (5) Å. [b] In II, the eight P–C bonds in the $(C_6H_5)_4P^+$ cations are within the range 1.780 (9)–1.808 (9) Å with a mean value of 1.792 (9) Å. The C–C bonds in the phenyl rings range from 1.323 (14) to 1.432 (15) Å with a mean value of 1.38 (2) Å. The C_i–P–C_j angles are found between 107.8 (4) and 111.7 (4)° with a mean value of 109.5 (4)°. [c] For the cation in III, the N–C bonds are within the range 1.43 (3)–1.60 (3) Å with a mean value of 1.52 (4) Å. [d] In IV, the N–C bonds in the nondisordered cation (N1) range from 1.49 (2) to 1.54 (2) Å with a mean value of 1.52 (2) Å and the C_i–N1–C_j angles range from 108 (1) to 111 (1)° with a mean value of 109 (1)°. In the disordered cation (N2), the range of the N–C bonds is from 1.45 (3) to 1.57 (4) Å with a mean value of 1.52 (4) Å. [e] In all cases, the standard deviations from the mean have been obtained as follows: $\sigma = [\sum_{i=1}^{N}(X_i - \bar{X})^2/N(N-1)]^{1/2}$. [f] The common labeling scheme for all anions is given in Figure 2.

$Fe_{24}S_{26}Cl$ (2.30 Å), and the $[Fe_8S_6I_8]^{3-}$ cluster (2.32 Å).[16,33] By comparison, the $\overline{Fe–S}$ bond lengths in the $[Fe_6S_6Cl_6]^{3-}$ and

(33) The Fe–S bonds in this structure have been reported to range from 2.309 (9) to 2.332 (10) Å.

Table X. ^{57}Fe Mössbauer Parameters for the $[Fe_6S_6X_6(Mo(CO)_3)_2]^{n-}$ (X = Cl⁻, Br⁻, I⁻) and the $[Fe_6S_6X_6]^{n-}$ Complexes (X = Cl⁻, Br⁻)

compd	T, K	$\delta,^a$ mm/s	ΔE_q, mm/s	Γ^-, mm/s	Γ^+, mm/s	Γ^+/Γ^-
$(Et_4N)_3Fe_6S_6Cl_6[Mo(CO)_3]_2$	80	0.584 (5)	1.080 (5)	0.386 (5)	0.376 (5)	0.99
$(Et_4N)_3Fe_6S_6Br_6[Mo(CO)_3]_2$	80	0.588 (5)	1.047 (5)	0.310 (5)	0.280 (5)	0.95
$(Ph_4P)_3Fe_6S_6I_6[Mo(CO)_3]_2$	127	0.56 (2)	1.00 (2)			
$(Et_4N)_4Fe_6S_6Cl_6[Mo(CO)_3]_2$	80	0.634 (5)	1.007 (5)	0.354 (5)	0.318 (5)	1.00
$(Et_4N)_4Fe_6S_6Br_6[Mo(CO)_3]_2$	80	0.613 (5)	0.992 (5)	0.372 (5)	0.372 (5)	1.00
$(Ph_4P)_2Fe_6S_6Cl_6$	80	0.455 (5)	0.725 (5)			
$(Ph_4P)_2Fe_6S_6Br_6$	80	0.460 (5)	0.717 (5)			
$(Et_4N)_3Fe_6S_6Cl_6{}^b$	125	0.495 (1)	1.085 (1)			
$(Et_4N)_3Fe_6S_6Br_6{}^b$	125	0.493 (1)	1.132 (1)			

^{a} Isomer shift with respect to iron metal at room temperature. ^{b} From ref 17c.

$[Fe_6S_6Cl_6]^{2-}$ prismanes are 2.276 (3) and 2.258 (8) Å. The mean value of the Fe–S bond length in $[Fe_6S_6I_6]^{2-}$ has also been reported at 2.257 (5) Å. Collectively, the Fe–S structural data for the various Fe_6S_6 cores show a small but gradual decrease in the bond lengths that parallels the increase of the *formal* oxidation states of the Fe atoms. These are +2.125 in $[Fe_6S_6I_6]^{3-}$, +2.33 in the $[Fe_6S_6X_6(Mo(CO)_3)_2]^{4-}$ adducts, ~+2.41 in $K_6LiFe_{24}S_{26}Cl^{30}$ and $(K_6Cl)_2[(Fe_8S_6)S_{8/3}]_6,^{31}$ +2.5 in the $[Fe_6S_6X_6]^{3-}$ prismanes,^{17} and +2.66 in the oxidized $[Fe_6S_6X_6]^{2-}$ prismanes.^{17} A similar trend is apparent in the Fe–Cl bond lengths. The latter, in I, III, the $[Fe_6S_6Cl_6]^{3-}$ cluster, and the $[Fe_6S_6Cl_6]^{2-}$ cluster are 2.245 (2), 2.225 (4), 2.224 (2), and 2.185 (5) Å, respectively. These small but apparently systematic changes are also apparent in the ^{57}Fe Mössbauer isomer shift values for these compounds (vide infra, Table X). The Fe–Fe distances in either the hexagonal or rhombic faces of the Fe_6S_6 cores in I–IV are found (Table IX) over a rather wide range, and the mean values are similar (within 1σ) to those in the parent prismanes.

A comparison of the Fe–Mo and Mo–S distances between I and II and between III and IV (Table IX) shows that, in the trianions (III and IV), these distances are slightly shorter and suggests that the LUMO in III and IV may have appreciable Mo bonding character. This is further substantiated by the considerable hypsochromic shifts in the C–O stretching vibrations in III and IV by comparison to those in I and II (Table VII). A partial oxidation of the Mo atoms in III and IV is also hinted at in the S–Mo–S angles. The latter, at 95.8 (1) and 95.2 (7)° in III and IV, are slightly larger than those in I and II (93.4 (4) and 93.9 (7)°).

The $S_3Mo(CO)_3$ structural units in the adducts display a pseudooctahedral electronic symmetry at the Mo atom and are structurally analogous to the corresponding unit in the tricarbonyl(1,4,7-trithiacyclononane)molybdenum(0) complex.^{23} In the latter, the Mo–S bonds are significantly shorter and range from 2.504 (6) to 2.543 (7) Å. The shorter $\overline{Mo-C}$ distances in I and II (Table IX), by comparison to the $\overline{Mo-C}$ distance^{34} in $Mo(CO)_6$ (2.06 (2) Å), indicate that the prismane "ligands" serve as π donors toward the Mo atoms in the tetraanionic adducts. The slightly longer Mo–C bonds in the trianionic III and IV are not unexpected, considering that, in the latter, the Mo atoms appear to be partially oxidized.

Electron Paramagnetic Resonance (EPR) and Mössbauer Spectra. The EPR spectra of the $[Fe_6S_6X_6(Mo(CO)_3)_2]^{n-}$ clusters were examined in the solid state and/or frozen CH_3CN solution. The tetraanionic clusters were found to be EPR-silent at 4.2 K and very likely possess an $S = 0$ ground state. The trianionic clusters, not unlike the $[Fe_6S_6X_6]^{3-}$ clusters, show a broad EPR signal at temperatures <25 K consistent with an $S = \frac{1}{2}$ ground state. Representative EPR spectra are shown in Figure 3. The spectra for the $[Fe_6S_6X_6(Mo(CO)_3)_2]^{3-}$ complexes (X = Cl⁻, I⁻) were simulated with the following parameters: X = Cl⁻, $g_1 = 1.350$, $g_2 = 1.936$, $g_3 = 2.051$; X = I⁻, $g_1 = 1.660$, $g_2 = 1.999$, $g_3 = 2.031$. In the simulation of the parent $[Fe_6S_6Cl_6]^{3-}$ prismane, the parameters obtained^{17c} were $g_1 = 1.20$, $g_2 = 1.71$, and $g_3 = 2.038$.

The Mössbauer spectra were obtained for the prismane adducts

at 80 K. The spectra were fitted with two Lorentzians in order to detect any significant asymmetry. The hyperfine parameters deduced from the fits are listed in Table X. Included in this table also are parameters for certain $[Fe_6S_6(L)_6]^{n-}$ anions.

Previous analyses of Mössbauer results on biologically occurring or synthetic analogue Fe/S clusters^{35} have established an empirical linear relationship between the value of the isomer shift and the average oxidation state of the Fe ions. From the values of isomer shifts for Fe^{3+} and Fe^{2+} ions with tetrahedral sulfur coordination (0.25 and 0.7 mm/s, respectively), one can deduce a value of 0.45 mm/s for a valence change of 1. This value may change somewhat if the type of ligands changes, but this is a second-order effect as long as tetrahedral coordination is maintained. Under this assumption, the expected change as one goes from the prismane dianion to the trianion would be (1/6)0.45 or 0.075 mm/s. The observed change (Table X) of 0.05 mm/s may be an indication that part of the charge goes to the ligands. In the $[Fe_6S_6X_6(Mo(CO)_3)_2]^{3-}$ trianions, an increase in the isomer shift by ~0.07 mm/s, by comparison to the corresponding $[Fe_6S_6X_6]^{3-}$ trianions, may be considered an indication that a unit of charge has been transferred to the core from the two $Mo(CO)_3$ units. Reduction of the trianion adducts by one electron leads to an increase of the isomer shift by only ~0.035 mm/s. Apparently, the reduction affects the Mo atoms to a significant extent. The Mössbauer results^{35b} further reinforce earlier conclusions that were based on crystallographic and infrared spectroscopic data. These are as follows. (a) The Fe_6S_6 cores in either of the two oxidation levels of the $[Fe_6S_6X_6(Mo(CO)_3)_2]^{n-}$ adducts are reduced by nearly one electron when compared to the Fe_6S_6 cores in $[Fe_6S_6X_6]^{3-}$. (b) Oxidation–reduction of the adducts is centered primarily on the Mo atoms.

Summary and Conclusions

The $[Fe_6S_6X_6(Mo(CO)_3)_2]^{n-}$ clusters represent a new entry to a class of heterometallic Fe/Mo/S clusters that have been obtained in attempts toward the synthesis of an analogue for the Fe/Mo/S center in nitrogenase. Other members in this general class include (a) the double cubanes $[Mo_2Fe_6S_9(SR)_8]^{3-},^{36,37}$ $[Mo_2Fe_6S_8(SR)_9]^{3-,4-},^{38}$ $[Mo_2Fe_6S_8(OMe)_3(SR)_6]^{3-},^{37}$ $[Mo_2Fe_6S_8(SEt)_3(OPh)_6]^{3-},^{37d}$ $[M_2Fe_7S_8(SR)_{12}]^{3-,4-},^{38a}$ and $[M_2Fe_6S_8(SR)_6(3,6-R_2cat)_2]^{4-},^{39}$ (b) the single-cubane clusters that include $[MFe_3-$

(34) Beach, N. A.; Gray, H. B. *J. Am. Chem. Soc.* **1968**, *90*, 5713.

(35) (a) Christou, G.; Mascharak, P. K.; Armstrong, W. H.; Papaefthymiou, G. C.; Frankel, R. B.; Holm, R. H. *J. Am. Chem. Soc.* **1982**, *104*, 2820. (b) A detailed study of the magnetic properties and the magnetically perturbed Mössbauer spectra of the $[Fe_6S_6(X)_6(Mo(CO)_3)_2]^{3-}$ complexes will be reported elsewhere.

(36) Wolff, T. E.; Berg, J. M.; Warrick, C.; Hodgson, K. O.; Holm, R. H.; Frankel, R. B. *J. Am. Chem. Soc.* **1978**, *100*, 4630.

(37) (a) Acott, S. R.; Christou, G.; Garner, C. D.; King, T. J.; Mabbs, F. E.; Miller, R. E. *Inorg. Chim. Acta* **1979**, *35*, L337. (b) Christou, G.; Garner, C. D.; Mabbs, F. E. *Inorg. Chim. Acta* **1978**, *28*, L189. (c) Cleland, W. E.; Averill, B. A. *Inorg. Chim. Acta* **1985**, *107*, 187.

(38) (a) Wolff, T. E.; Power, P. P.; Frankel, R. B.; Holm, R. H. *J. Am. Chem. Soc.* **1980**, *102*, 4694. (b) Christou, G.; Garner, C. D. *J. Chem. Soc., Dalton Trans.* **1980**, 2354.

(39) (a) Armstrong, W. H.; Holm, R. H. *J. Am. Chem. Soc.* **1981**, *103*, 6246. (b) Armstrong, W. H.; Mascharak, P. K.; Holm, R. H. *J. Am. Chem. Soc.* **1982**, *104*, 4373.

(40) (a) Palermo, R. E.; Singh, R.; Bashkin, J. K.; Holm, R. H. *J. Am. Chem. Soc.* **1984**, *106*, 2600–2612. (b) Mascharak, P. K.; Armstrong, W. H.; Mizobe, Y.; Holm, R. H. *J. Am. Chem. Soc.* **1983**, *105*, 475.
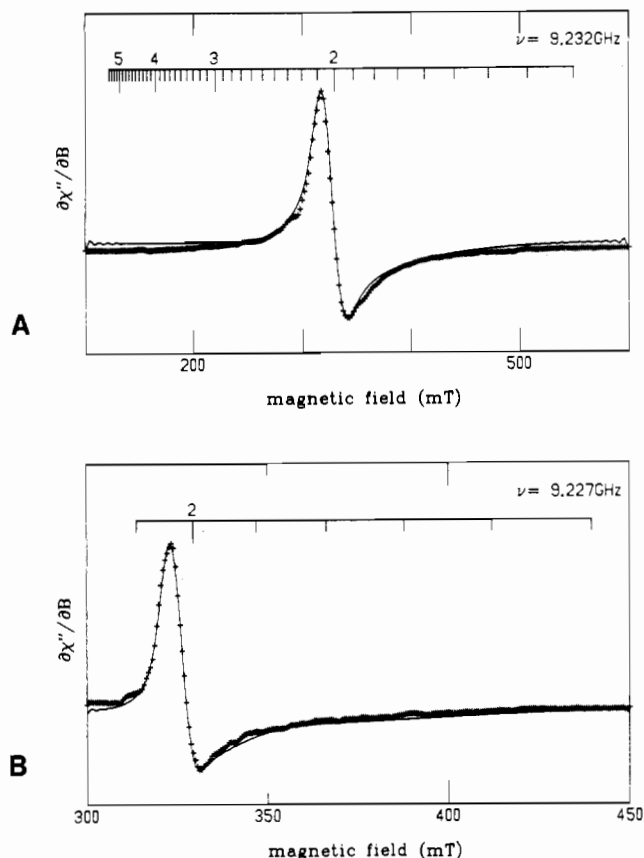
Figure 3. Observed and simulated EPR spectra: (A) $[(C_2H_5)_4N]_3Fe_6-S_6Cl_6[Mo(CO)_3]_2$, solid, 21 K, microwave frequency 9.232 GHz; (B) $[(C_6H_5)_4P]_3Fe_6S_6I_6[Mo(CO)_3]_2$, frozen CH_3CN (0.24 mM) solution, 8 K, microwave frequency 9.227 GHz.

$(S)_4(SR)_3(3,6-R_2cat)L]^{2-,3-}$ [40] (L = p-$ClC_6H_4S^-$, THF, N_3^-, and CN^-) and $[MoFe_3(S)_4(SEt)_3Fe(cat)_3]^{3-}$,[41] (c) oligonuclear complexes, derivatives of the MS_4^{2-} thioanions[14] that include $[L_2FeS_2MS_2]^{2-}$ (L = PhS^-;[42] L = Cl^-,[43] PhO^-,[44] NO^+;[45] $L_2 = S_5^{2-}$[46]), $[Cl_2FeS_2MS_2FeCl_2]^{2-}$,[43,47] $[Fe(MoS_4)_2]^{3-}$,[48] $[Fe(WS_4)_2-(DMF)_2]^{2-}$,[49] $[(S_2)OMoS_2FeCl_2]^{2-}$,[50] $[S_2MoS_2FeS_2Fe(S-p-C_6H_4Me)_2]^{3-}$,[44,51] $[Mo_2FeS_6(edt)_2]^{3-}$,[52] and $[(S_2WS_2)_3Fe_3S_2]^{4-}$.[53]

(41) Wolff, T. E.; Berg, J. M.; Holm, R. H. *Inorg. Chem.* **1981**, *20*, 174.
(42) (a) Coucouvanis, D.; Simhon, E. D.; Swenson, D.; Baenziger, N. C. *J. Chem. Soc., Chem. Commun.* **1979**, 361. (b) Tieckelmann, R. H.; Silvis, H. C.; Kent, T. A.; Huynh, B. H.; Waszczak, J. V.; Teo, B. K.; Averill, B. A. *J. Am. Chem. Soc.* **1980**, *102*, 5550.
(43) (a) Coucouvanis, D.; Baenziger, N. C.; Simhon, E. D.; Stremple, P.; Swenson, D.; Simopoulos, A.; Kostikas, A.; Petrouleas, V.; Papaefthymiou, V. *J. Am. Chem. Soc.* **1980**, *102*, 1732. (b) Müller, A.; Tolle, H. G.; Bogge, H. *Z. Anorg. Allg. Chem.* **1980**, *471*, 115.
(44) Silvis, H. C.; Averill, B. A. *Inorg. Chim. Acta* **1981**, *54*, L57.
(45) Coucouvanis, D.; Simhon, E. D.; Stremple, P.; Baenziger, N. C. *Inorg. Chim. Acta* **1981**, *53*, L135.
(46) Coucouvanis, D.; Baenziger, N. C.; Simhon, E. D.; Stremple, P.; Swenson, D.; Kostikas, A.; Simopoulos, A.; Petrouleas, V.; Papaefthymiou, V. *J. Am. Chem. Soc.* **1980**, *102*, 1730.
(47) Müller, A.; Sarkar, S.; Domrose, A. M.; Filgueira, R. *Z. Naturforsch.* **1980**, *35B*, 1592.
(48) (a) Coucouvanis, D.; Simhon, E. D.; Baenziger, N. C. *J. Am. Chem. Soc.* **1980**, *102*, 6644. (b) McDonald, J. W.; Friesen, G. D.; Newton, W. E. *Inorg. Chim. Acta* **1980**, *46*, L79. (c) Müller, A.; Hellmann, W.; Schneider, J.; Schimanski, U.; Demmer, U.; Trautwein, A.; Bender, U. *Inorg. Chim. Acta* **1982**, *65*, L41. (d) Friesen, G. D.; McDonald, J. W.; Newton, W. E.; Euler, W. B.; Hoffman, B. M. *Inorg. Chem.* **1983**, *22*, 2202.
(49) Stremple, P.; Baenziger, N. C.; Coucouvanis, D. *J. Am. Chem. Soc.* **1980**, *102*, 4601.
(50) Müller, A.; Sarkar, S.; Bogge, H.; Jostes, R.; Trautwein, A.; Lauer, U. *Angew. Chem., Int. Ed. Engl.* **1983**, *22*, 747.
(51) Tieckelman, R. H.; Averill, B. A. *Inorg. Chim. Acta* **1980**, *46*, L35.
(52) Dahlstrom, P. L.; Kumar, S.; Zubieta, J. *J. Chem. Soc., Chem. Commun.* **1981**, 411.
(53) Müller, A.; Hellmann, W.; Bogge, H.; Jostes, R.; Romer, M.; Schimanski, U. *Angew. Chem., Int. Ed. Engl.* **1982**, *21*, 860; *Angew. Chem. Suppl.* **1982**, 1757.

and (d) derivatives of the $[Fe_2S_2(CO)_6]^{2-}$ dianion in reactions with $MoCl_5$ that include the $[MoOFe_5S_6(CO)_{12}]^{2-}$ cluster.[54]

The structures of the above complexes can be described in terms of either FeS_2Mo or FeS_2Fe units. The latter structural description seems to be acceptable also for the Fe/Mo/S center in nitrogenase and derives from Mo and Fe EXAFS studies.[9-11] With the possible exception of the $[MoOFe_5S_6(CO)_{12}]^{2-}$ anion, none of the *structurally characterized* synthetic Fe/Mo/S clusters adhere to the stoichiometry of the Fe/Mo/S center in nitrogenase. Nevertheless, various synthetic clusters display certain electronic or structural characteristics that resemble those known for the Fe/Mo/S site in nitrogenase. The single-cubane clusters with the $MoFe_3(S)_4$ cores appear to be the most successful synthetic analogues as far as spectroscopic characteristics are concerned. In particular, these compounds are characterized by $S = ^3/_2$ ground states and show Mo X-ray absorption spectra[55] and EXAFS quite similar to those of the Fe/Mo/S site in nitrogenase. The major argument against virtually all known synthetic Fe/Mo/S clusters as acceptable analogues emerges from their stoichiometry. In comparison to the case for the nitrogenase center or the Fe/Mo cofactor, these complexes still do not have the low (1:(7 ± 1)) Mo:Fe ratio and the apparent inequivalency of iron sites suggested by Fe EXAFS,[10,11] ENDOR,[5] and Mössbauer spectroscopic studies.[3,4]

The prismane adducts reported herein possess a Mo:Fe stoichiometry of 1:3, magnetic ground states $S = ^1/_2$ and $S = 0$ for the 3– and 4– levels, respectively, and structural features that only qualitatively resemble the Fe/Mo/S site in nitrogenase. The large size of the highly reduced Mo atom in I–IV results in Fe–Mo and Mo–S distances (Table IX) that are considerably longer than those found by EXAFS in nitrogenase and the nitrogenase cofactor. Similarly, the Fe–Fe distances in the synthetic clusters are distinctly longer (by ca. 0.1 Å) than the Fe–Fe distances in the nitrogenase cofactor, obtained by Fe EXAFS analyses and reported independently by two groups at 2.66[10] and 2.63 Å.[11]

The molecular and electronic structural differences notwithstanding, the $[Fe_6S_6X_6(Mo(CO)_3)_2]^{n-}$ clusters still appear promising as a source for stoichiometrically and electronically acceptable synthetic analogues. Currently, we are exploring the feasibility of synthesizing derivative clusters of the type $[Fe_6S_6X_6(MoL_3)]^{n-}$ with a 1:6 Mo:Fe ratio and the Mo in a higher oxidation state. The latter with an $MoFe_6S_6$ core (Figure 1B) would be similar to a model suggested previously[15a] (Figure 1A) as a possible structural analogue for the nitrogenase Fe/Mo site and should be chemically accessible by the oxidative decarbonylation of the $[Fe_6S_6X_6(Mo(CO)_3)]^{n-}$ 1:1 adducts. Evidence for the presence of the latter has been obtained from the isotropically shifted ^1H NMR spectra of the $[Fe_6S_6(OAr)_6(Mo(CO)_3)_2]^{3-}$ adducts in CH_3CN solution.[18a,56] The spectra clearly show the dissociation of $Mo(CO)_3$ from the 2:1 adducts according to the equilibrium

$$[Fe_6S_6(OAr)_6(Mo(CO)_3)_2]^{3-} \rightarrow$$
$$[Fe_6S_6(OAr)_6(Mo(CO)_3)]^{3-} + (CH_3CN)_3Mo(CO)_3$$
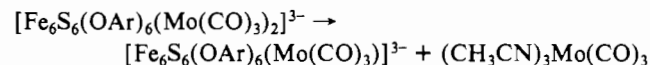
Ongoing studies in our laboratory are aimed toward the isolation of the 1:1 adducts employing specifically designed tripodal ligands capable of spanning and coordinating to the three Fe atoms within one of the hexagonal faces of the prismane clusters. The specific sequestering of three of the four terminal coordination sites in the Fe_4S_4 clusters with a "cavitant" ligand has already been reported.[57]

A structural feature unique to the prismanes and the Mo prismane adducts is an Fe–Fe distance of ∼3.8 Å between the Fe atoms in the hexagonal Fe_3S_3 chairs. An indication of a second shell of Fe atoms at a distance of ∼3.65 Å was reported in the most recent Fe EXAFS study[11] of the Fe/Mo/S center in nitrogenase. Thus far, we have been unable[58] to detect this second

(54) Bose, K. S.; Lamberty, P. E.; Kovacs, J. E.; Sinn, E.; Averill, B. A. *Polyhedron* **1986**, *5*, 393.
(55) Conradson, S. D. Ph.D. Thesis, Stanford University, 1983.
(56) Coucouvanis, D.; Al-Ahmad, S.; Salifoglou, A., manuscript in preparation.
(57) Stack, T. D. P.; Holm, R. H. *J. Am. Chem. Soc.* **1987**, *109*, 2546.
(58) Cramer, S., private communication.

shell of Fe atoms in the Fe EXAFS of the $[Fe_6S_6(L)_6(Mo(C-O)_3)_2]^{n-}$ adducts.

Notes

Contribution from the Department of Chemistry,
University of Utah, Salt Lake City, Utah 84112

Protic Acid Behavior of Phosphine–Triborane(7)

Rosemarie E. DePoy and Goji Kodama*

The protic acid behavior of phosphine–borane(3) ($BH_3 \cdot PH_3$) has been demonstrated by its reaction with ammonia to give $NH_4^+[BH_3 \cdot PH_2]^{-1,2}$ and by its reaction with $NaBH_4$ in dimethoxyethane at 0 °C to produce hydrogen gas and $Na^+[BH_3 \cdot PH_2 \cdot BH_3]^{-}.^3$ In the reaction with ammonia a further change occurs at a higher temperature (–45 °C) to finally give an ammonium salt of the $[BH_3 \cdot PH_2 \cdot BH_3]^-$ anion.^{1,2}

The observed enhanced protonic character of the PH_3 hydrogen atoms is due to the coordination of a BH_3 fragment to the PH_3. Since the B_3H_7 fragment is a stronger acid than BH_3,^{4,5} phosphine–triborane(7) ($B_3H_7 \cdot PH_3$) is expected to behave as a stronger protic acid than $BH_3 \cdot PH_3$. Conversely, the conjugate base $[B_3H_7 \cdot PH_2]^-$ should be weaker than $[BH_3 \cdot PH_2]^-$. In this paper, the reactions of $B_3H_7 \cdot PH_3$ with ammonia and with $NaBH_4$ are described and compared with those of $BH_3 \cdot PH_3$ in order to delineate the similarities and differences between the acid–base reaction chemistries of $B_3H_7 \cdot PH_3$ and $BH_3 \cdot PH_3$.

Results

A. Formation of $[B_3H_7 \cdot PH_2]^-$. $B_3H_7 \cdot PH_3$ in Liquid Ammonia. In Figure 1, the ^{11}B and ^{31}P NMR spectra of a liquid ammonia solution of $B_3H_7 \cdot PH_3$ (ca. 0.5 M) are shown and compared with those of $B_3H_7 \cdot PH_3$ in dichloromethane. The ^{31}P spectra indicated that, upon dissolution of $B_3H_7 \cdot PH_3$ in liquid ammonia, the PH_3 moiety of the molecule was converted to a PH_2^- unit: the ^{31}P signal is a 1:2:1 triplet of a 1:1:1:1 quartet. The ^{11}B spectra indicated that the B_3H_7 group remained intact: the two ^{11}B signals appear in a 2:1 intensity ratio. These spectra remained unchanged as long as the solution was kept below –45 °C. When the solvent ammonia was removed by pumping, the original $B_3H_7 \cdot PH_3$ was recovered as residue. Thus, the following equation is appropriate for the interaction of $B_3H_7 \cdot PH_3$ with ammonia:

$$B_3H_7 \cdot PH_3 + NH_3 \rightleftharpoons NH_4^+ + [B_3H_7 \cdot PH_2]^- \qquad (1)$$

At –45 °C, the solute underwent a slow change to give the $[B_3H_7 \cdot PH_2 \cdot BH_3]^-$ anion (see part B of this section) and as yet unidentified species indicated by the ^{11}B signals at –15 and –48 ppm.

Isolation of the Sodium Salt of $[B_3H_7 \cdot PH_2]^-$. Phosphine–triborane(7) could be deprotonated by the use of $Na^+[HB(sec\text{-}Bu)_3]^-$ (eq 2 and 3). The salt $Na^+[B_3H_7 \cdot PH_2]^-$, which was soluble in

$$B_3H_7 \cdot PH_3 + Na^+[HB(sec\text{-}Bu)_3]^- \xrightarrow{-45\ °C\ \text{in THF}}$$
$$Na^+[B_3H_7 \cdot PH_2 \cdot B(sec\text{-}Bu)_3]^- + H_2 \quad (2)$$

$$Na^+[B_3H_7 \cdot PH_2 \cdot B(sec\text{-}Bu)_3]^- \xrightarrow{-B(sec\text{-}Bu)_3/\text{pumping}}$$
$$Na^+[B_3H_7 \cdot PH_2]^- + B(sec\text{-}Bu)_3 \quad (3)$$

(1) Gilje, J. W.; Morse, K. W.; Parry, R. W. *Inorg. Chem.* **1967**, *6*, 1761.
(2) Dietz, E. A.; Morse, K. W.; Parry, R. W. *Inorg. Chem.* **1976**, *15*, 1.
(3) Mayer, E.; Laubengayer, A. W. *Monatsh. Chem.* **1970**, *101*, 1138.
(4) Edwards, L. J.; Parry, R. W. *J. Am. Chem. Soc.* **1959**, *81*, 3554.
(5) Bishop, V. L.; Kodama, G. *Inorg. Chem.* **1981**, *20*, 2724.
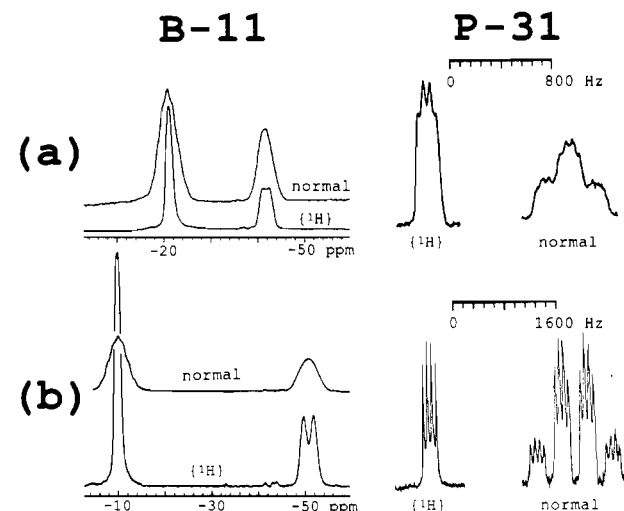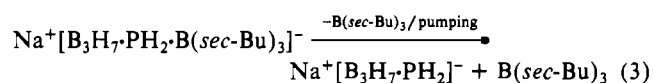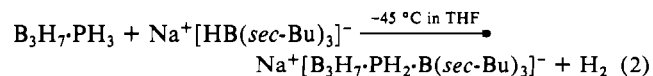
Figure 1. ^{11}B and ^{31}P NMR spectra (32.1 and 40.5 MHz, respectively) of $B_3H_7 \cdot PH_3$ (a) in ammonia at –70 °C and (b) in CH_2Cl_2 at +25 °C, recorded on a Varian XL-100-15 spectrometer.
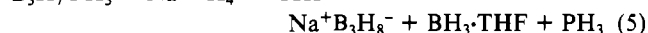
tetrahydrofuran and dichloromethane, could be isolated as a white solid by pumping out the solvent and $B(sec\text{-}Bu)_3$ from the reaction mixture below –45 °C. The major features of the NMR spectra of $Na^+[B_3H_7 \cdot PH_2]^-$ are identical with those of the ammonia solution of $B_3H_7 \cdot PH_3$ in Figure 1. The spectral data of this anion and its related compounds are summarized in Table I. Treatment of a solution of this salt with anhydrous hydrogen chloride regenerated $B_3H_7 \cdot PH_3$. The $B_3H_7 \cdot PH_2^-$ anion decomposed above –45 °C to form the $[B_3H_7 \cdot PH_2 \cdot BH_3]^-$ anion and another unidentified species, which showed a broad ^{11}B signal ($\nu_{1/2} = 250$ Hz) centered at –35.5 ppm.

Several attempts were made to prepare the salts of the $[B_3H_7 \cdot PH_2]^-$ anion by other methods, which included treatments of ammonia solutions of $B_3H_7 \cdot PH_3$ with sodium metal and with $NaNH_2$, treatment of $B_3H_7 \cdot PH_3$ with n-butyllithium in hexane, and treatment of $B_3H_7 \cdot THF$ with KPH_2 in diglyme. These attempts, however, were unsuccessful. Apparently, the B_3H_7 moiety undergoes reactions with these reagents. The $B_3H_7 \cdot PH_2^-$ ion could be detected only in the ^{11}B NMR spectrum of the $NaNH_2$ reaction solution (usually in <40% yields). It, however, could not be isolated from the product mixture.

B. Formation of $[B_3H_7 \cdot PH_2 \cdot BH_3]^-$. Phosphine–triborane(7) reacted with $NaBH_4$ in tetrahydrofuran at –45 °C according to eq 4. The product $Na^+[B_3H_7 \cdot PH_2 \cdot BH_3]^-$, a white solid, was very

$$B_3H_7 \cdot PH_3 + Na^+BH_4^- \rightarrow Na^+[B_3H_7 \cdot PH_2 \cdot BH_3]^- + H_2 \qquad (4)$$

soluble in tetrahydrofuran, and was stable at room temperature in the absence of air. The anion $[B_3H_7 \cdot PH_2 \cdot BH_3]^-$ was inert toward strong Lewis bases, as prolonged contact with $P(CH_3)_3$ at ambient temperature left the anion unchanged.

The formation of the $[B_3H_7 \cdot PH_2 \cdot BH_3]^-$ anion was accompanied by a side reaction that produced NaB_3H_8 (eq 5). At –45 °C the

$$B_3H_7 \cdot PH_3 + Na^+BH_4^- + THF \rightarrow$$
$$Na^+B_3H_8^- + BH_3 \cdot THF + PH_3 \qquad (5)$$

participation of this side reaction was slight. At higher temperatures, however, it became increasingly significant. When